Paleozoic structural controls on shortening transfer in the Subandean foreland thrust system, Ene and southern Ucayali basins, Peru

Nicolas Espurt, Stéphane Brusset, Patrice Baby, Wilber Hermoza, Rolando Bolaños, Dennys Uyen, Joachim Déramond

Paleozoic structural controls on shortening transfer in the Subandean foreland thrust system, Ene and southern Ucayali basins, Peru

Nicolas Espurt,[1,2] Stéphane Brusset,[1] Patrice Baby,[1] Wilber Hermoza,[3,4] Rolando Bolaños,[3] Dennys Uyen,[5] and Joachim Déramond[1]

Received 26 November 2007; revised 14 February 2008; accepted 19 March 2008; published 20 June 2008.

[1] The Neogene evolution of the Ene and southern Ucayali basins of the Subandes has been controlled by two stacked thrust wedges that differ in terms of tectonic styles. The lower thrust wedge is formed by deep-seated décollements within the basement related to thick-skinned foreland structures inherited from an Early Carboniferous thrust system. Seismic reflection data show that this Paleozoic compressional system has been eroded and unconformably covered by Late Carboniferous clastic sediments. It generated an irregular Paleozoic sedimentary architecture controlling the Neogene thrust propagation. The upper thin-skinned thrust wedge developed within this Paleozoic sedimentary series and constitutes the Subandean zone. Cross-section balancing shows an along-strike homogenous horizontal shortening of ~56 km (~30%) across the Ene–southern Ucayali thrust system. This amount of shortening was vertically partitioned onto the two stacked thrust wedges. The N-S thickness variations of the Paleozoic sedimentary prism controlled the eastward propagation of the upper thrust wedge. The southern thickening of the Paleozoic series generated major décollements and the shortening excess is of 7 km (16%) in comparison to the north. Consequently, the northern lack of shortening onto the upper thrust wedge was transferred to the Early Carboniferous compressional structures of the lower thrust wedge. We suggest that this vertical partitioning of the shortening was accommodated by a regional oblique ramp: the Tambo transfer zone. This geometrical analysis of the Ene–southern Ucayali thrust system provides new perspectives for future hydrocarbon exploration in this region. **Citation:** Espurt, N., S. Brusset, P. Baby, W. Hermoza, R. Bolaños, D. Uyen, and J. Déramond (2008), Paleozoic structural controls on shortening transfer in the Subandean foreland thrust system, Ene and southern Ucayali basins, Peru, *Tectonics*, *27*, TC3009, doi:10.1029/2007TC002238.

1. Introduction

[2] The knowledge of the Paleozoic framework (variable thickness of the basins, thrust faults or basement highs) along the Andean orogen is fundamental to deciphering their implications in the structural architecture and kinematics evolution of the Subandean zone deformation [e.g., *Baby et al.*, 1994; *Colletta et al.*, 1997; *Alvarez-Marron et al.*, 2006; *Vergés et al.*, 2007]. The along-strike accommodation of the deformation through these inherited structures is often considered as one of the important factors explaining the development of oblique ramp with shortening transfer [e.g., *Thomas*, 1990; *Marshak and Wilkerson*, 1992; *Calassou et al.*, 1993; *Baby et al.*, 1994; *Corrado et al.*, 1998; *Marques and Cobbold*, 2002].

[3] Transfer zones have been defined by *Dahlstrom* [1969] as zones where the shortening is transferred from one structure to another, resulting in lateral variations in the thrust system geometry. This mechanism has been described in many frontal regions of foreland thrust systems [e.g., *Baby et al.*, 1992; *Calassou et al.*, 1993; *Baby et al.*, 1994; *Wang*, 1997; *Mueller and Talling*, 1997; *Philippe et al.*, 1998; *Corrado et al.*, 1998; *Mouthereau et al.*, 1999; *Wilkerson et al.*, 2002; *Hinsch et al.*, 2002; *Soto et al.*, 2002; *Ravaglia et al.*, 2004; *McClelland and Oldow*, 2004; *Mon et al.*, 2005], but never in the Peruvian Subandean zone, even if the traces of frontal thrusts are very irregular (Figure 1) [*Mégard*, 1978; *Kley et al.*, 1999; *Gil Rodriguez et al.*, 2001; *Cobbold et al.*, 2007].

[4] The Ucayali basin is located in the southwestern corner of the northern Amazonian foreland basin [*Roddaz et al.*, 2005] which overlies the Nazca Ridge flat slab segment (Figure 1) [*Gutscher et al.*, 1999]. The Ucayali Subandean zone (Figure 1) has developed since the Middle Miocene (15–10 Ma) [*Hermoza et al.*, 2005] and is still in progress [*Dorbath*, 1996]. The northern Ucayali Subandean zone (Pachitea basin) is NNW-SSW trending (Figures 1 and 2). It is mainly related to tectonic inversions of Permian-Triassic grabens which started in Late Cretaceous times [*Baby et al.*, 1999; *Gil Rodriguez et al.*, 2001; *Hermoza et al.*, 2005]. In contrast, the southern Ucayali Subandean zone (Ene and Camisea basins) exhibits typical curved thrust structures which interfere with inherited basement highs of

[1]Laboratoire des Mécanismes et Transferts en Géologie, Université de Toulouse, CNRS, IRD, OMP, Toulouse, France.
[2]Now at Institut Français du Pétrole, Rueil-Malmaison, France.
[3]PERUPETRO S.A., Lima, Peru.
[4]Now at REPSOL-YPF, Madrid, Spain.
[5]PLUSPETROL E&P S.A., Lima, Peru.

0278-7407/08/2007TC002238

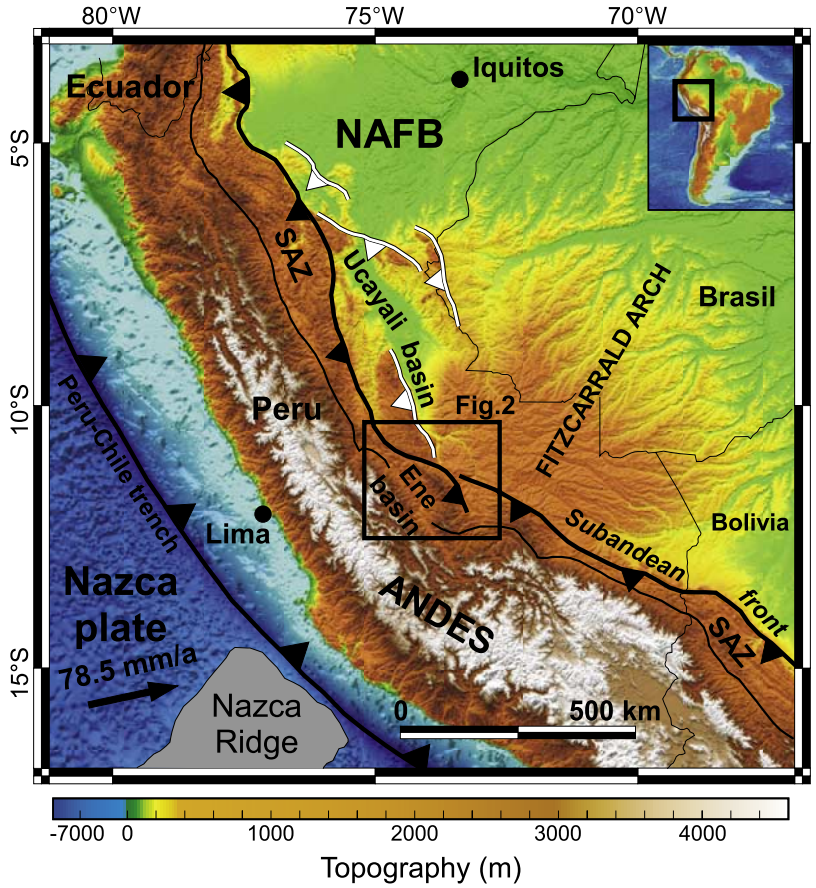

Figure 1. Geodynamic setting of the central Andes. The Ene and Ucayali basins are located on the eastern side of the Andes in the northern Amazonian foreland basin (NAFB) [*Roddaz et al.*, 2005] and north of the Fitzcarrald Arch [*Espurt et al.*, 2007]. The base map is produced using bathymetric data from the Geosat and ERS-1 spacecraft [*Smith and Sandwell*, 1997] and elevation data from NASA SRTM Gtopo 30. Plate convergence vector is from *Gripp and Gordon* [2002]. White lines with triangles show thick-skinned thrusts in the foreland basin. Black square indicates the study area shown in Figure 2. SAZ, Subandean zone.

the foreland (Figures 1 and 2) [*Dumont et al.*, 1991; *Kley et al.*, 1999]. In the Ene basin, this interference induced a conspicuous NW–SE trending fault system, named the Tambo fault system [*Mégard*, 1978], oblique to the ENE trending regional shortening (Figure 2). Because of its location, this oblique thrust system is expected to play an important role in the evolution of the Subandean fold-and-thrust belt and should be an area of main interest for future hydrocarbon exploration. Its southern prolongation corresponds to the large structural traps of the giant gas/condensate province of the Camisea basin (Figure 2) [*Chung et al.*, 2006].

[5] This paper aims to describe the structural architecture, kinematics and mechanism of the deformation of the Ene and southern Ucayali basins from new surface and subsurface data. Two regional balanced cross sections are presented to analyze, geometrically and quantitatively, the Subandean deformation in order to understand the origin of the oblique Tambo thrust system. Relationships between thrust system lateral evolution and location of structural traps are then discussed.

2. Geological Setting

2.1. Tectonics Units

[6] The Ucayali basin extends between 7° and 12° South latitudes on the eastern side of the Peruvian Andes (Figure 1). It belongs to the northern Amazonian foreland basin [*Roddaz et al.*, 2005] on the northern flank of the Fitzcarrald Arch [*Espurt et al.*, 2007]. The southern edge of the Ucayali basin (Figures 2 and 3a) displays a complex structural architecture with an eastern Ucayali zone including basement-involved thrusts (thick-skinned tectonic style in the sense of *Kley et al.* [1999]), such as the Shira mountain [*Dumont et al.*, 1991; *Gil Rodriguez*, 2002] and the Sepa anticline, and a western Subandean zone where only the sedimentary cover is involved in the deformation (thin-

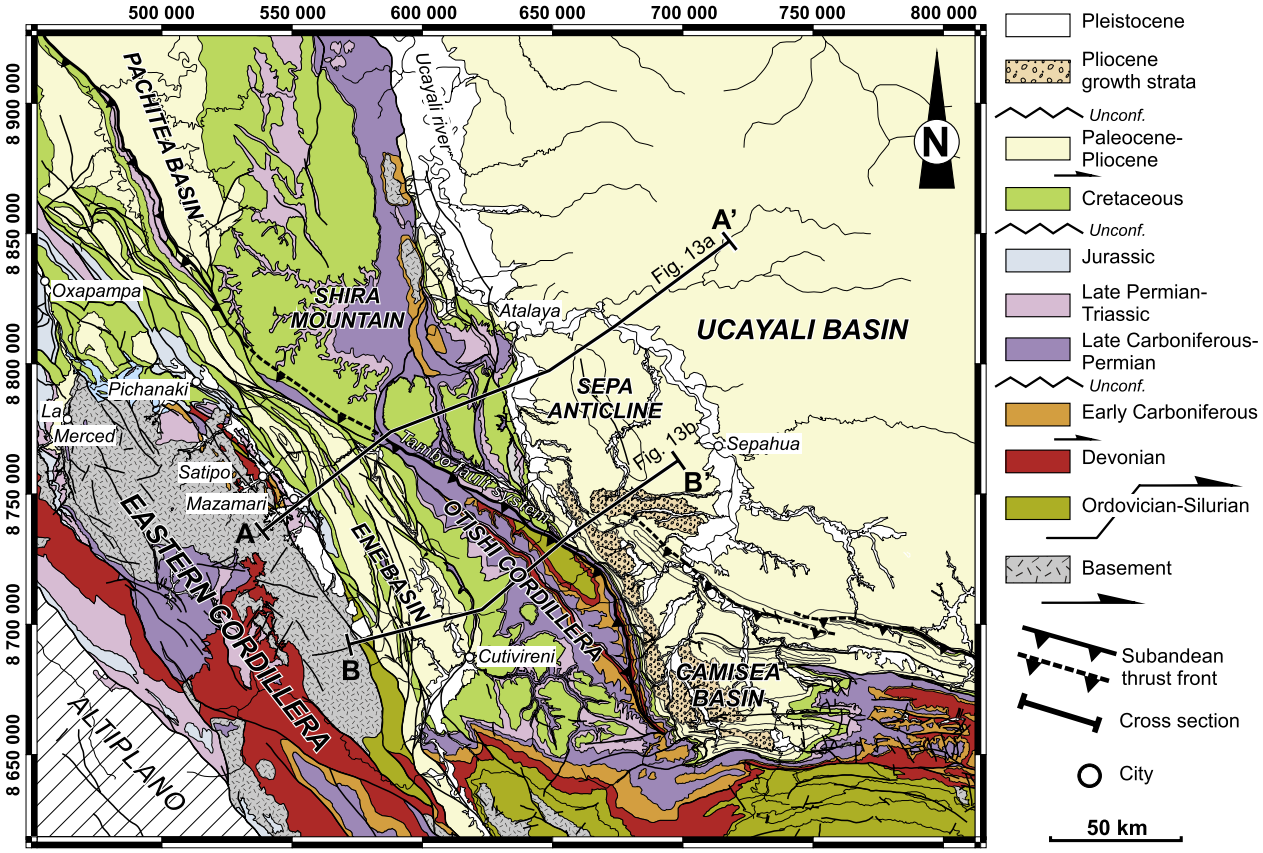

Figure 2. Geologic map of the study area. The main morphotectonic units described in the text are shown. The location of the two balanced cross sections of Figure 13 are shown.

skinned tectonic style in the sense of *Kley et al.* [1999]). The Subandean zone comprises three main morphotectonic units (Figures 2 and 3a): the Camisea basin, the Otishi Cordillera and the Ene basin. The southeastern Camisea basin corresponds to thrust-related long wavelength anticlines [*Bellido*, 1969; *Dumont et al.*, 1991; *Mathalone and Montoya*, 1995; *Shaw et al.*, 1999]. The Camisea basin includes the giant gas/condensate province [*Chung et al.*, 2006]. The Otishi Cordillera is characterized by curve-shaped thrust trajectories. The western Ene basin is constituted by closely spaced imbricated thrusts. To the west, the Subandean zone is overthrust by the Eastern Cordillera. Thus, the Ene-Ucayali thrust system is dominated by a hybrid thin- and thick-skinned tectonic style as described in many foreland thrust systems [e.g., *Kley*, 1996; *Kley et al.*, 1999; *Lacombe and Mouthereau*, 2002; *Giambiagi et al.*, 2003; *McQuarrie*, 2004; *Sherkati et al.*, 2005], involving Paleozoic to Tertiary strata and propagating through a heterogeneous mechanical stratigraphy inherited from pre-Andean paleogeography [*Gil Rodriguez et al.*, 2001].

2.2. Regional Stratigraphy

[7] The basement is made up of igneous rocks and Paleozoic metasediments, and outcrops in the Eastern Cordillera (Merced dome) and on the eastern flank of the Shira mountain (Figure 2) [*Mégard*, 1978]. It is overlain by a heterogeneous sedimentary series ranging from Ordovician to Pleistocene. The sedimentary series may be divided into four distinct stratigraphic units delimited by regional unconformities (Figure 3b).

2.2.1. Ordovician to Early Carboniferous

[8] The oldest unit corresponds to a Paleozoic southwest thickening wedge formed by Ordovician to Early Carboniferous rocks (Figure 3a). Thick Ordovician-Silurian strata outcrop in the western edge of the Ene basin and on the eastern side of the Otishi Cordillera (Figures 2 and 3b). They correspond to the black shales, sandstones and quartzites of the Ananea, San Gaban, San José and Sandia formations [*Benavides*, 1956; *Wilson and Reyes*, 1964; *Mégard*, 1978]. Devonian rocks consist of thick turbidites, shallow marine and fluvial/deltaic sandstones of the Cabanillas formation. They are overlain by Early Carboniferous shales and coarse-grained sandstones of the Ambo formation [*Newell et al.*, 1953]. In the Shira mountain, the oldest sedimentary formations pinchout on the basement rocks. Ordovician to Early Carboniferous rocks were deformed during the Paleozoic [*Mégard*, 1978].

2.2.2. Late Carboniferous to Jurassic

[9] The basal part of the second unit is formed by Late Carboniferous green sandstones and limestones of the Tarma formation [*Dunbar and Newell*, 1946] which unconformably overlie the previous unit (Figure 3a). The Tarma

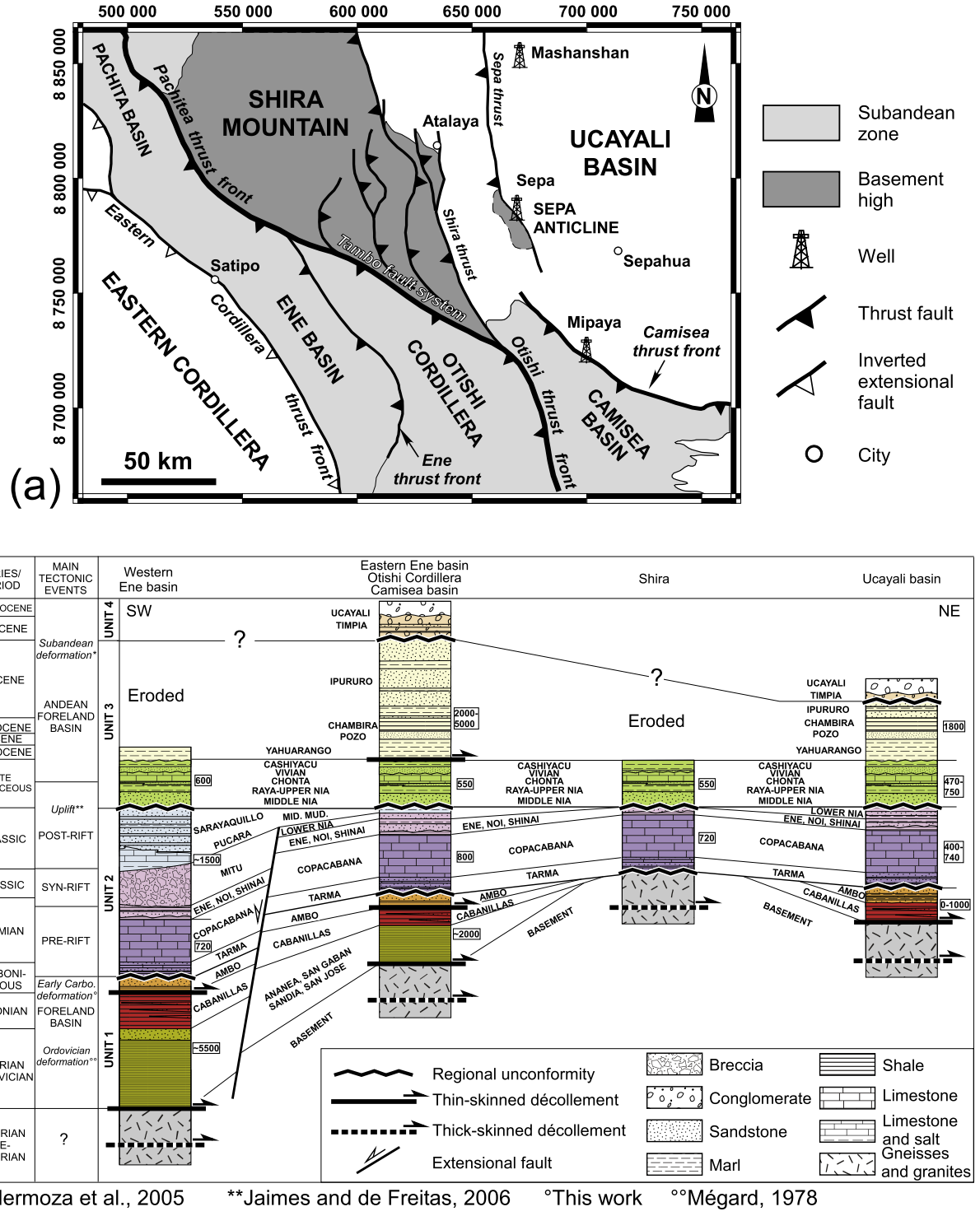

(b)

Figure 3. (a) Structural map of the study area. (b) Synthetic stratigraphic columns from the western Ene basin to the Ucayali basin. Thicknesses of the sedimentary formations are shown.

formation is covered by uniformly thick Permian marine limestones of the Copacabana formation [*Cabrera La Rosa and Petersen*, 1936] widely exposed in the Shira mountain and the Otishi Cordillera (Figure 2) [*Mégard*, 1978]. These shelf series are successively overlain by dolostones interbedded with black marine shales of the Ene formation, fluvial/aeolian sandstones of the Noi formation and red marls of the Shinai formation.

[10] Permian-Triassic rift sequences are essentially preserved in the western side of the Ene basin where they filled the Oxapampa-Satipo half-graben (Figures 2, 3a, and 3b). Permian-Triassic red rocks correspond to the massive breccias and evaporites of the Mitu formation [*Newell et al.*, 1953] deposited during the rifting event and period of intense volcanism and plutonism [*Capdevila et al.*, 1977; *Dalmayrac et al.*, 1980; *Soler and Bonhomme*, 1990].

[11] Jurassic deposits consist in the basal limestones, dolomites and evaporites of the Pucara formation [*Szekely and Grose*, 1972; *Rosas et al.*, 2007] deposited on a shelf during postrift, and upper fluvial rocks of the Sarayaquillo formation [*Koch*, 1962; *Mégard*, 1979].

[12] Eastward, Permian-Jurassic relics (<50 m thick) corresponding to the aeolian sandstones of the lower Nia formation and Middle Mudstones formation [*Chung et al.*, 2006] are preserved below the Cretaceous unconformity [*Mégard*, 1978].

2.2.3. Late Cretaceous to Miocene

[13] The third sedimentary unit (Figure 3a) is underlined by the basal Late Cretaceous middle Nia formation [*Chung et al.*, 2006] which consists in thick coarse sandstones corresponding to amalgamated braided channel fills. Upward, it is overlain by the marine shales of the Raya formation, sandstones of the upper Nia formation, marine carbonate mudstones of the Chonta formation [*Kummel*, 1948; *Seminario and Guizado*, 1976], massive sandstones of the Vivian formation [*Seminario and Guizado*, 1976; H. Müller and E. Aliaga, Estudio bioestratigrafico del Cretaceo de la Cuenca Marañon, unpublished report, 1981], and finally by marls and calcarenites of the Cashiyacu formation (Müller and Aliaga, unpublished report, 1981).

[14] The Late Cretaceous section is conformably covered by Paleocene to Miocene series (Figure 3a). The Paleocene–Early Eocene Yahuarango formation [*Kummel*, 1948; M. Gutiérrez, Zonacion bioestratigrafica del intervalo Cretaceo superior–Terciario inferior, in Evaluacion del potencial de las Cuencas Huallaga, Ucayali y Madre de Dios, unpublished report, 1982] comprises red and purple clays with rich nodular carbonate layers and gypsum. The Eocene-Oligocene Pozo formation [*Kummel*, 1948; *Williams*, 1949] is made up of olive green and greenish gray, fine grained, silty, micaceous claystone, and friable sandstones. Lithic sandstone beds and thick interbedded conglomerate channels become more common upward into the Oligocene–Early Miocene Chambira formation [*Kummel*, 1948]. Finally, the Miocene Ipururo formation [*Kummel*, 1948] consists of greyish to brownish sandstones interbedded with reddish silts [*Hermoza et al.*, 2005].

2.2.4. Pliocene to Pleistocene

[15] The Pliocene Timpia terrestrial formation (V. Graterol Airborne gravity and magnetic survey. Block 52, Ucayali basin, Peru, unpublished report, 1998) of the upper unit (Figure 3a) consists of syntectonic series with growth stratal pattern deposited during the Subandean deformation. In the Camisea basin (Figures 2 and 3b), these deposits organize in eastward prograding alluvial fans which are aligned on the eastern side of the Otishi Cordillera. These deposits consist of conglomerates, with very minor medium gray to greyish orange sandstone, ranging from matrix-supported to clast-supported, with clasts of quartzite, sandstone, limestone, granite and andesite of variable size ranging from pebbles to boulders (V. Graterol, unpublished report, 1998). The Pleistocene Ucayali formation [*Kummel*, 1948] consists in aggradational terraces of conglomerates filling the incised valleys.

2.3. Décollement Levels

[16] On a regional scale, four potential décollement levels are determined from the mechanical stratigraphy. The structural highs which developed in the Ucayali basin are controlled by décollement in the basement, proved by basement rock exposures on the eastern flank of the Shira mountain (Figures 2 and 3b) [*Mégard*, 1978] and by seismic reflection data (see below). The basement-Paleozoic sediments interface is interpreted as a main décollement horizon [*Gil Rodriguez*, 2002] within the Subandean zone. In the Ene basin, the shortening is accommodated by shallower alternative mechanical weakness zones. An intermediate décollement is located in the shales of the Ambo formation (Early Carboniferous) and an upper décollement at the Cretaceous-Paleocene sediments interface (Figures 3a and 6).

3. Surface and Subsurface Structural Data

[17] Surface data were obtained from 1:100,000 INGEMMET (Instituto Nacional Geológico, Minero y Metalúrgico del Peru) geologic maps, PERUPETRO S.A. geologic data, digital elevation models from SRTM data, LANDSAT images, and also from several field surveys carried out in 2005 and 2006 in this area. Subsurface data consist of unpublished well and seismic reflection data provided by PERUPETRO S.A. These data have been used to interpret the structure at depth and the geometry of the thrust systems.

3.1. Subandean Zone

3.1.1. Ene Basin

[18] The Ene basin is a NW–SE trending feature of about 40 km wide and 180 km long, with an average elevation of ~900 m (Figures 2 and 4). It is overthrust by the Merced dome made up of igneous rocks, Paleozoic sediments, and minor Mesozoic and Cenozoic strata [*Soler and Bonhomme*, 1987; *Laubacher and Naeser*, 1994]. The surface geometry of the northern Ene basin along the Satipo river (Figures 4a and 4b) corresponds to two wide synclines (Tziriari and Tarobeni synclines) filled by thick Cenozoic series bounded

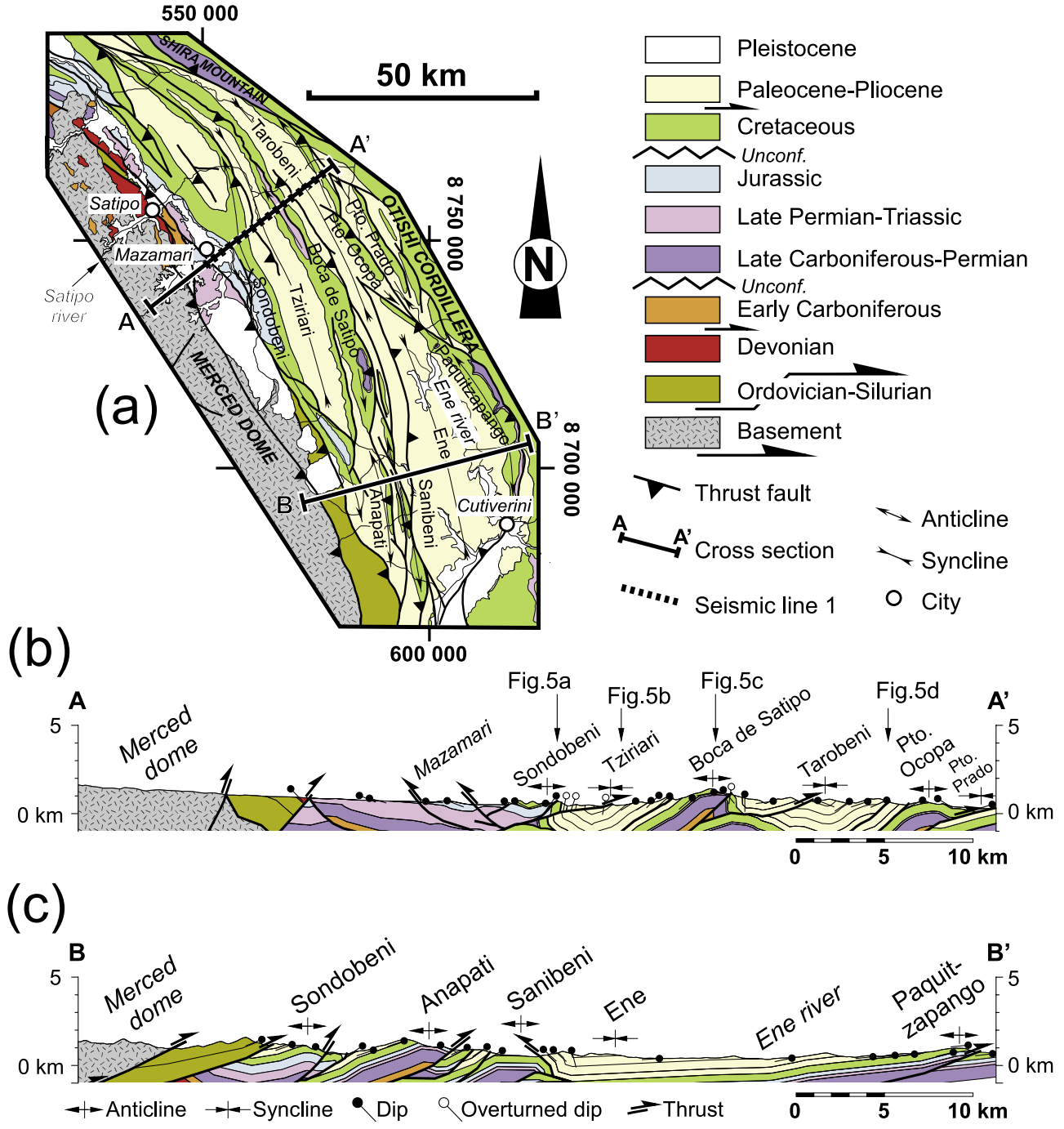

Figure 4. (a) Geologic map of the Ene basin, and surface cross sections across (b) the northern and (c) southern Ene basin. Cross sections are also indicated in Figure 2. Location of seismic line 1 of Figure 6 is shown.

by three east-verging thrust-related anticlines (Sondobeni, Boca de Satipo and Puerto Ocopa anticlines). The western Mazamari unit is formed by 15°–20° east-dipping Permian-Cretaceous strata warped by a set of west-verging thrusts (Figure 4b). Eastward, these strata are involved in the Sondobeni breakthrough fault-propagation fold [*Suppe and Medwedeff*, 1990; *Mitra*, 1990]. This anticline is characterized by a 40°–50° west-dipping backlimb and an overturned forelimb (Figure 5a), which dips 80°–85° westward (Figure 4b). The lower thrust associated to the Sondobeni anticline cuts the prestructured Cenozoic series of the Tziriari syncline (Figure 4b and Figure 5b) characterizing an out-of-sequence kinematics. The rapid westward stratigraphic thickening of the Permian-Triassic series

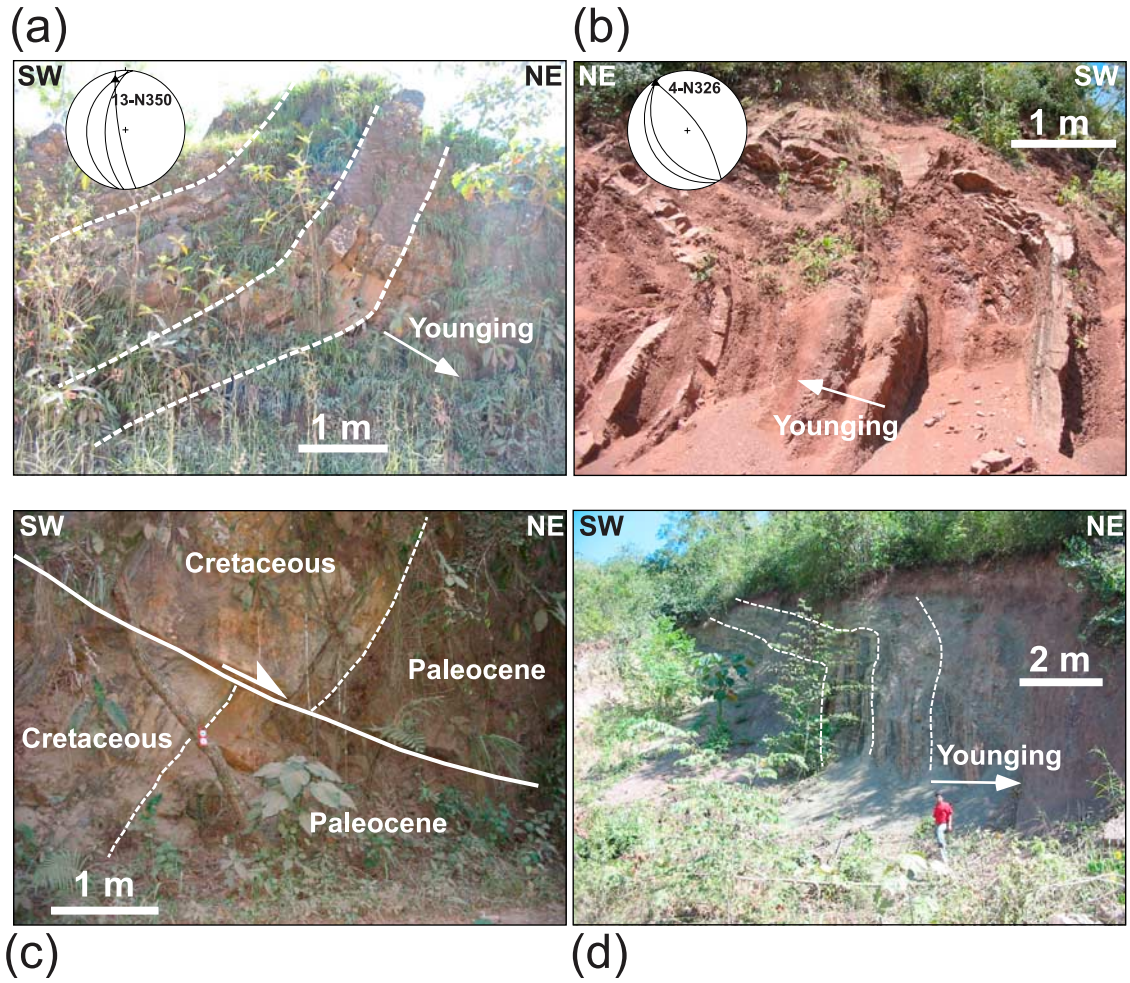

Figure 5. Deformation styles in the northern Ene basin along the Satipo river. For location, see Figures 4a and 4b. (a) Overturned and folded Cretaceous strata of the Sondobeni anticline (11.29466°S, 74.45031°W). (b) Fold in the Cenozoic strata of the Tziriari syncline (11.25214°S, 74.42554°W). (c) Overturned and sheared Cretaceous and Paleocene strata of the Boca de Satipo anticline (11.21133°S, 74.38789°W). (d) Fold in the Cenozoic strata of the Tarobeni syncline (11.17676°S, 7434996°W). These outcrop-scale folds indicate shallower second-order décollements which accommodated the shortening of deeper structures. Stereographic projections of the fold axis are shown.

shows that the Sondobeni thrust results from tectonic inversion of an extensional structure (Oxapampa-Satipo). Such an inversion occurred along the western edge of the Ene basin. Thus, the rectilinear geometry of the Eastern Cordillera thrust front (Figure 4a) can be explained by the tectonic inversion of an eastern rift boundary, assuming the extensional fault was rectilinear. Eastward, the Tziriari syncline is transported on the hanging wall of the Boca de Satipo thrust system (Figure 4b). The Boca de Satipo thrust system is associated with an upper broad fault-propagation fold which exhibits a 40°–50° west-dipping hanging wall flat at the base of the Ambo formation shales. The hanging wall ramp consists in overturned Cretaceous to Paleocene strata dipping 70°–85° westward (Figure 5c). To the east, the lower thrust associated with the Boca de Satipo anticline cuts and deforms Cenozoic strata of the Tarobeni syncline (Figures 4b and 5d). The overturned forelimbs and cores of the Sondobeni and Boca de Satipo anticlines were intensively sheared (Figures 5a and 5c). The Puerto Ocopa anticline corresponds to a major east-verging fault-bend fold overthrusting Paleocene strata of the easternmost Puerto Prado syncline (Figures 4a and 4b). The anticline displays a backlimb dipping 20°–25° westward and a forelimb dipping 30° eastward (Figure 4b). The thrust-related Puerto Ocopa anticline dips 10°–15° eastward, parallel to Paleocene bedding planes of the footwall.

[19] The deep structure of the northern Ene basin is illustrated by the SW–NE trending seismic reflection line 1 (Figures 4a and 6). This profile was calibrated using surface data from ELF [*Ballard et al.*, 1997; *Houzay and Sejourne*, 1997; *Jaffuel*, 1997] and our fieldwork data. The seismic profile reveals that the Ene basin is detached above the

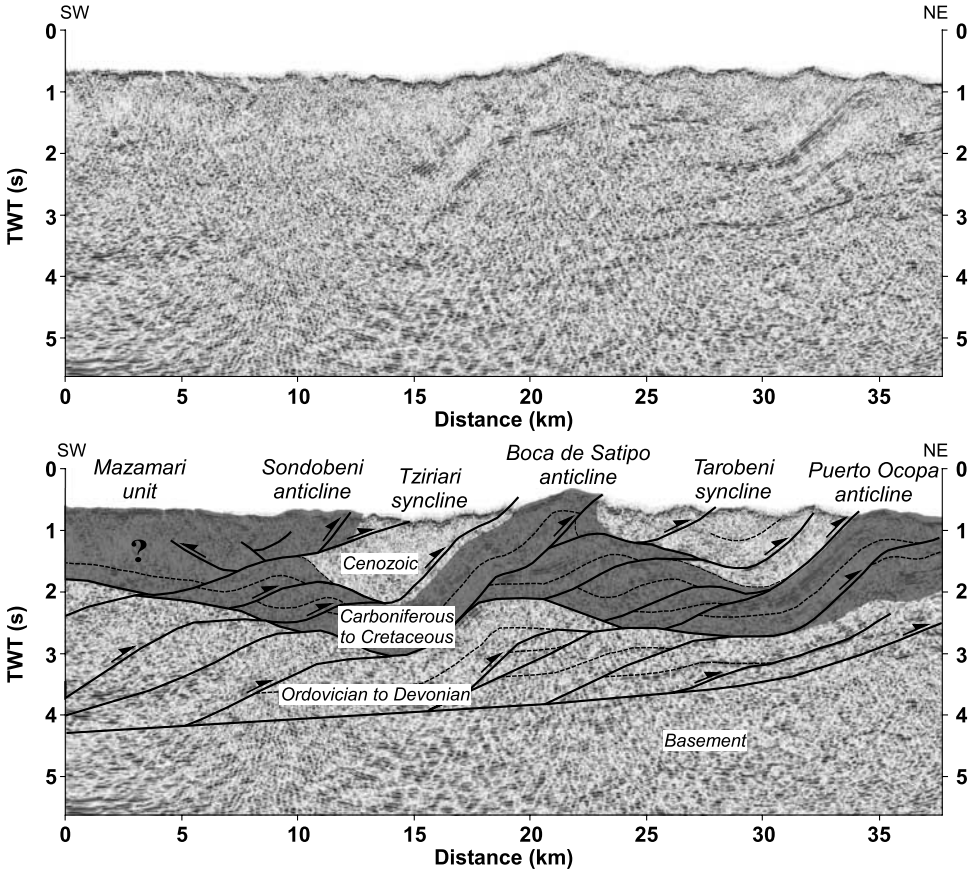

Figure 6. Structural interpretation of seismic line 1 across the northern Ene basin along the Satipo river. For location, see Figures 2 and 4a. Faults are indicated by thick black lines. Note the basement-Paleozoic series interface décollement dip increases under the Puerto Ocopa anticline. An intermediate décollement is located in the Early Carboniferous Ambo formation and an upper décollement near the Cretaceous-Paleocene sediments interface. TWT, two-way time.

décollement located at the basement-Paleozoic (Ordovician-Devonian) sediments interface (Figure 6). This décollement is connected through ramps to the intermediate décollement at the base of the Early Carboniferous shales of the Ambo formation and to the upper décollement at the Cretaceous-Paleocene rocks interface. The Sondobeni and Boca de Satipo anticlines are located above two major duplexes formed by several horses involving strata from Ordovician to Devonian. These two duplexes have accommodated the shortening within the Tziriari and Tarobeni synclines (Figure 6). The structure of the eastern Puerto Ocopa anticline is well delineated by reflectors. At depth, the fault plane dips 40°–45° westward and branches onto the intermediate décollement. The footwall ramp of the Puerto Ocopa thrust shows strata dipping ~20° westward.

[20] Southward, field and satellite imagery data indicate that the Ene basin is wider and differently deformed than in the north (Figures 4a and 4c). To the west, the structural geometry corresponds to three east-verging closely spaced thrust-related anticlines (Sondobeni, Anapati and Sanibeni anticlines). To the east, this thrust system is bounded by the asymmetrical and wide Ene syncline. Eastward, it is bounded by the Paquitzapango fault-bend fold. Along the Ene river, the backlimb of this anticline dips 15°–20° westward and the core of the fold exposes the upper part of Permian Copacabana limestones (Figure 4a). The Paquitzapango thrust cuts through the Mesozoic strata of the eastern Otishi Cordillera (Figures 4a and 4c). The thrust probably connects at depth with the intermediate décollement constituted by the shales of Early Carboniferous Ambo formation.

3.1.2. Otishi Cordillera

[21] The Otishi Cordillera is a main curve-shaped range (Figures 2 and 7) of about 60 km wide with a maximum elevation peaking at about 3500 m. To the north, the Otishi Cordillera overthrusts the southern edge of the Shira mountain. This zone corresponds to the Tambo fault system [*Mégard*, 1978], oblique to the ENE-regional tectonic transport direction (Figures 2 and 7a).The northern edge of the Otishi Cordillera is reduced to a ~30° west-dipping segment (Figures 7a and 7b) armed of thick limestones of the Permian Copacabana formation (Figure 8). Southward, the structure of the Otishi Cordillera consists in a broad

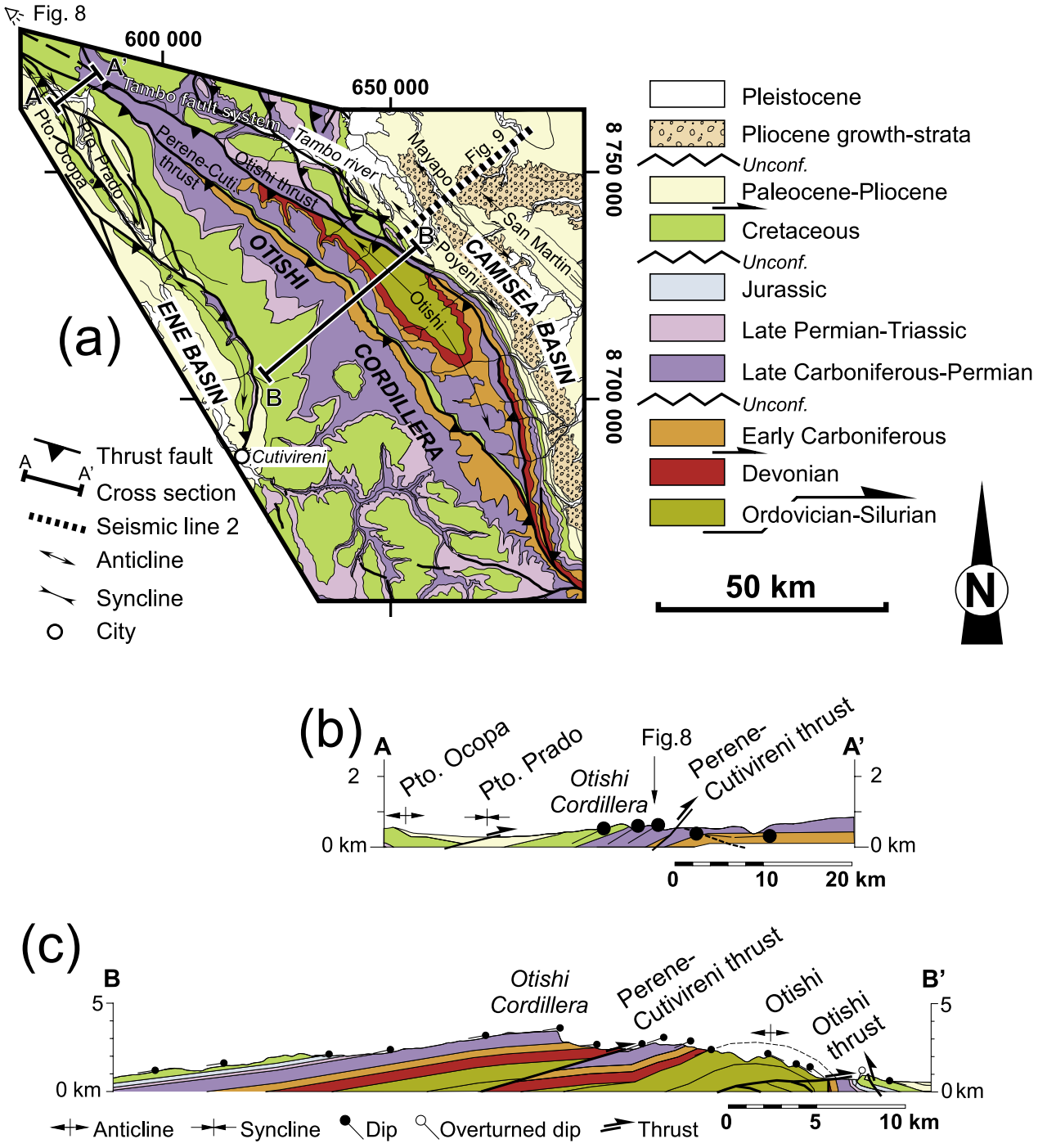

Figure 7. (a) Geologic map of the Otishi Cordillera and the northern edge of the Camisea basin. Surface cross sections across (b) the northern edge and (c) central part of the Otishi Cordillera. Note the bigger scale of the section A-A′ for more details. Location of seismic line 2 of Figure 9 is shown. For location, see also Figure 2.

~8° west-dipping homocline (Figures 7a and 7c). This homocline is truncated by the Perene-Cutivireni thrust which results in the duplication of the Permian Copacabana limestones and the high structural relief of the Otishi Cordillera (Figure 7c). It is easterly bounded by the broad Otishi anticline. The backlimb dips ~25° westward and the forelimb at ~30° eastward. The Otishi anticline overthrusts overturned Paleozoic and Mesozoic strata dipping ~80° southwestward (Figure 7c).

3.1.3. Camisea Basin

[22] On the eastern flank of the Otishi Cordillera, the northern Camisea thrust system consists in three east-

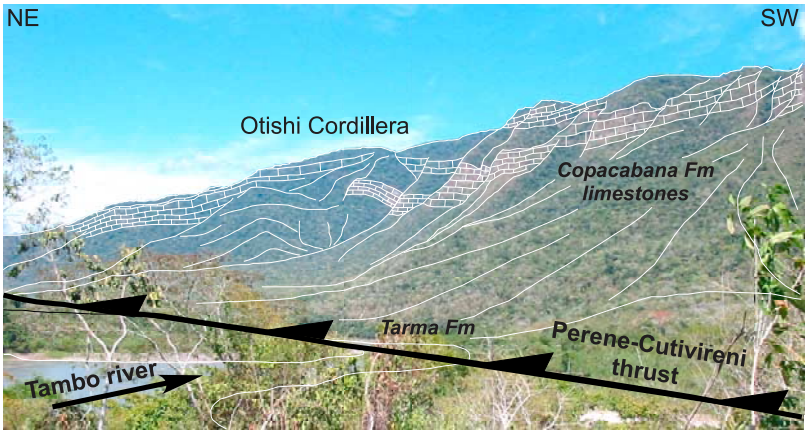

Figure 8. Photograph of the northern Otishi Cordillera thrust front along the Tambo river (11.13256°S, 74.19080°W), looking southward. See location in Figures 7a and 7b.

verging thrust-related anticlines (Poyeni, Mayapo and San Martin anticlines) (Figures 2 and 7a). The deep structure of the northern Camisea basin is illustrated by the SW–NE trending seismic reflection line 2 (Figure 9). Reflectors have been calibrated using projected data of the southern Mipaya well onto the section. To the southwest, the Poyeni anticline (Figure 9) is formed above an east-verging blind thrust associated with two back-thrusts. To the northeast, the displacement above the San Martin thrust is associated with the Mayapo and San Martin anticlines (Figure 9). The

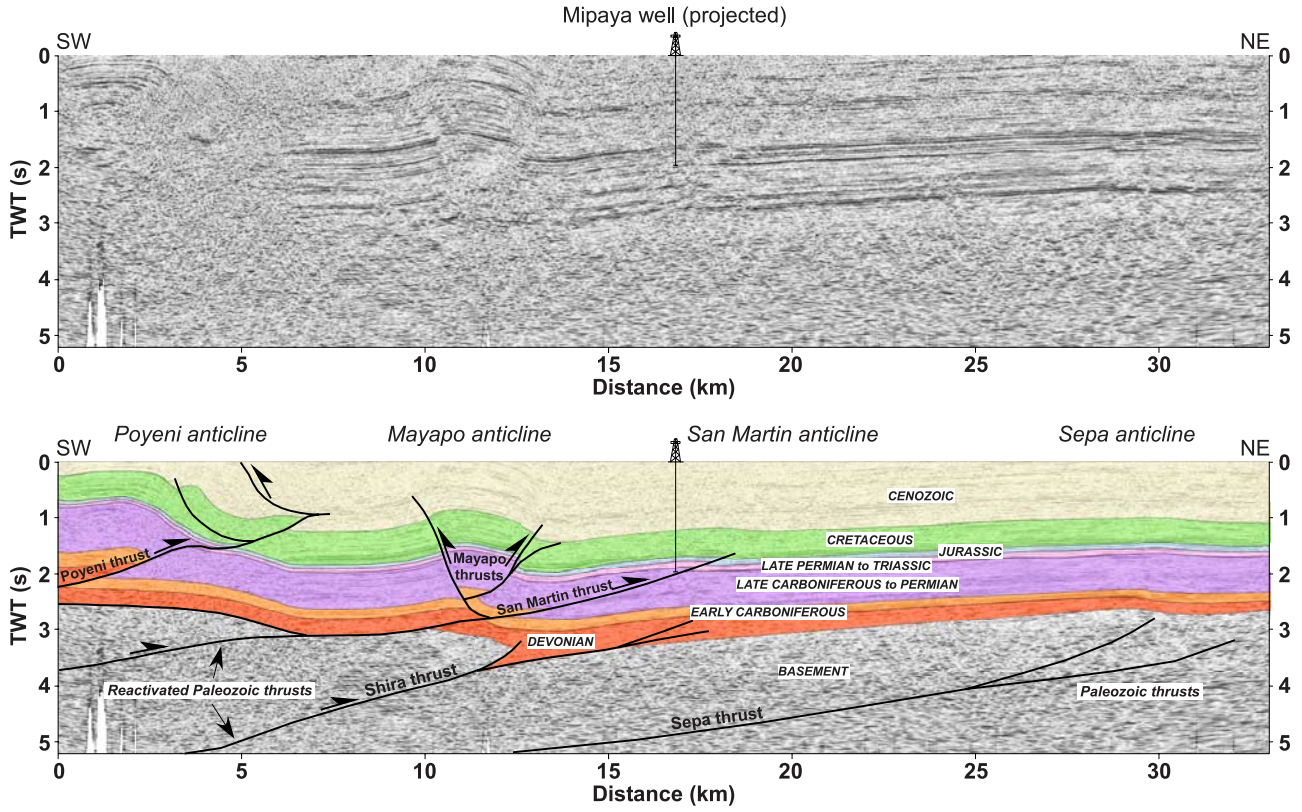

Figure 9. Interpretation of seismic line 2 across the northern edge of the Camisea basin. For location, see Figures 2 and 7a. The Camisea thrust system overlies thick-skinned thrusts of an Early Carboniferous thrust system. The reflectors have been calibrated using projected data of the southern Mipaya well (see location in Figure 18). Faults are indicated by thick black lines. TWT, two-way time.

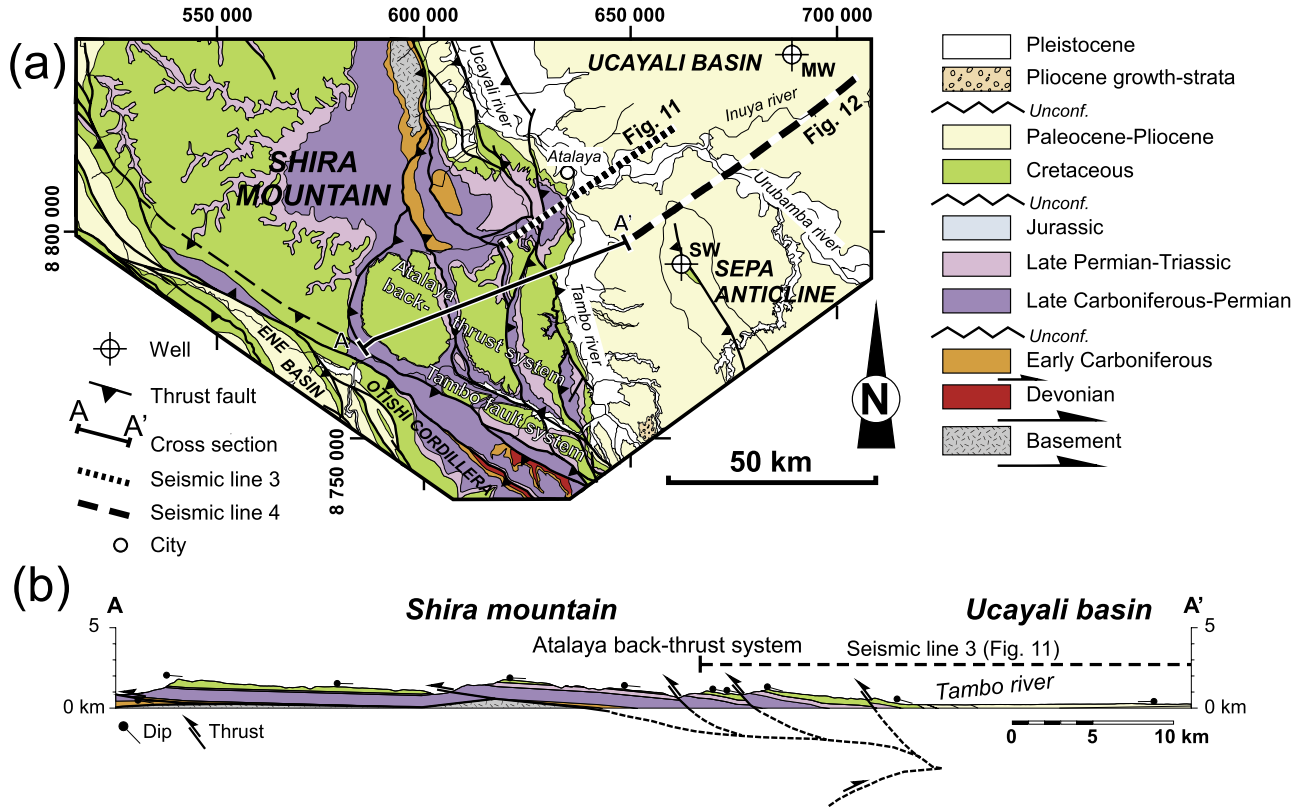

Figure 10. (a) Geologic map and (b) surface cross section across the southern Shira mountain. Location of seismic lines 3 and 4 of Figures 11 and 12, respectively, are shown. MW, Mashansha well; SW, Sepa well.

Mayapo anticline corresponds to a pop-up structure between two opposite verging blind thrusts. The thin-skinned thrust system branches to the décollement developed at the basement-Paleozoic sediments interface. The San Martin anticline is bounded to the east by the nonreactivated Sepa thick-skinned thrusts. The thick-skinned thrust system extends westward beneath the Otishi Cordillera (Figures 7a and 9).

3.2. Ucayali Basin

[23] The Ucayali basin exhibits NNE-SSW trending thick-skinned thrusts which deformed Mesozoic and Cenozoic strata of the Ucayali basin (Figures 2 and 10a) [*Räsänen et al.*, 1987; *Dumont et al.*, 1991]. To the west, the broad Shira mountain [*Dumont et al.*, 1991; *Gil Rodriguez*, 2002] is a N–S trending range of ~70 km wide and 270 km long (Figures 2 and 10a) with a maximum elevation reaching ~1400 m. Southward, the Shira mountain is bounded by the Tambo fault system (Figures 2 and 10a). The Shira mountain surface structure consists of five west-verging thrust sheets involving the sedimentary cover (Figure 10b), named the Atalaya back thrust system. Along the Tambo river valley, the westernmost thrust unit exhibits the horizontal strata of Tarma and Copacabana formations (Figure 10b). The easternmost thrust sheet shows Cretaceous strata dipping 10°–15° eastward.

[24] The eastern front of the southern Shira mountain is inferred from seismic line 3 (Figures 10a and 11). Its deep structure consists in eastward low-angle blind thick-skinned thrust within Devonian series of the Cabanillas formation. The westward Atalaya system of back-thrusts is mainly detached above the décollement located at the basement-Devonian sediments interface. This system of back-thrusts is the surface expression of the Shira thick-skinned thrusts emplacement at depth (Figure 11). The basement dips westward and forms the western limb of the Sepa anticline. The eastern flank of the Shira mountain shows warped Pliocene-Pleistocene (?) strata (Figure 11) which testify of a young activity the Shira thrust. The deformation style of the Shira mountain is similar to the one described by *Vergés et al.* [2007] for the Cerro Salinas thrust in Argentina (Sierras Pampeanas) where thick-skinned thrusts interfere in the Andean thrust front.

[25] The eastern broad Sepa anticline (Figures 2 and 10a) corresponds to a NNE–SSW trending bulge of ~100 km long and 70 km wide, located between the Tambo and Urubamba rivers. Late Cretaceous strata of the Vivian formation outcrop in the core of the fold (Figures 2 and 10a).

[26] The interpretation of seismic line 4 (Figures 10a and 12) is supported by well data (Sepa and Mashansha wells) projected onto the section. The Sepa anticline is formed

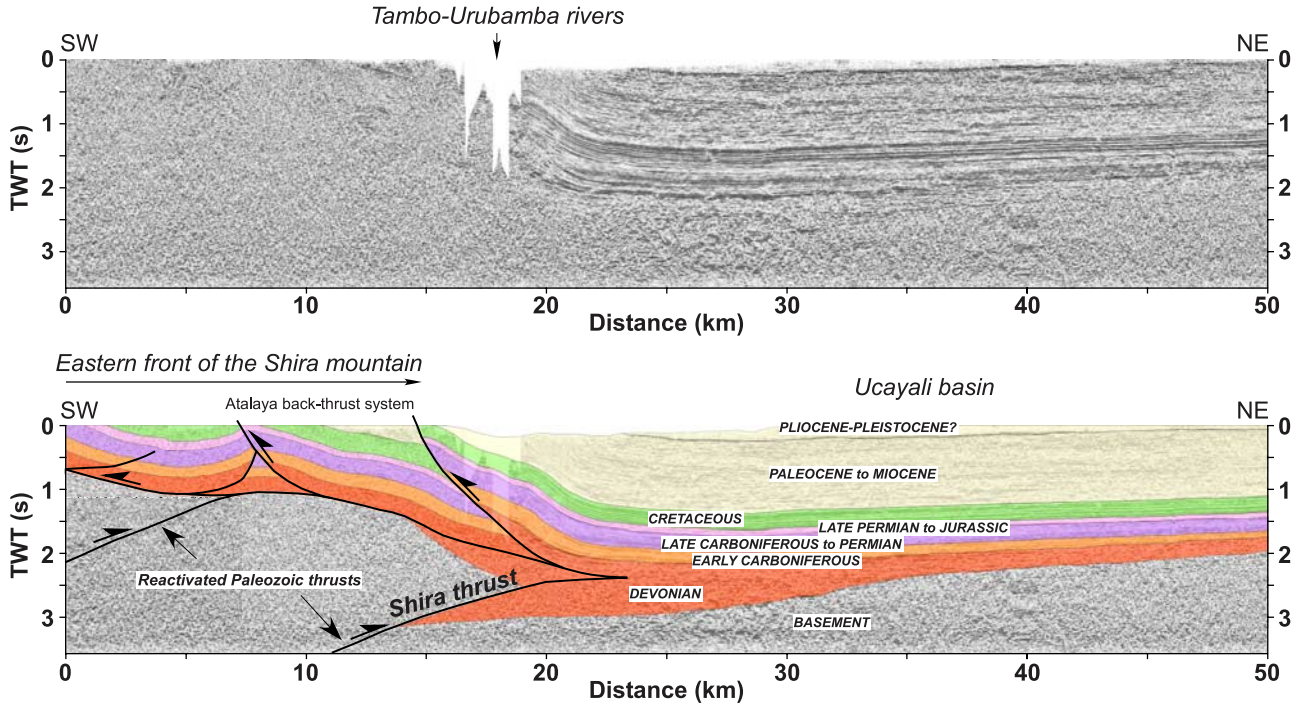

Figure 11. Interpretation of seismic line 3 across the eastern edge of the Shira mountain. For location, see Figures 2 and 10a. The reflectors have been calibrated using data of the Sepa and Mashansha wells. Faults are indicated by thick black lines. Note the thickness increase of the Devonian deposits in front of the Shira thrust front. TWT, two-way time.

above an east-verging low-angle thrust involving basement. The thrust branches upward into two blind thrusts. To the east, the Paititi high structure (Figure 12a) exhibits similar east-verging low-angle thick-skinned thrusts, which are sealed by the Late Carboniferous unconformity. Depositional thickness of the Paleozoic series increases westward, toward the Sepa and Paititi high thrusts, respectively (Figure 12a). The eastern limb of the Paititi high shows evidence of growth strata in the Early Carboniferous Ambo formation being deposited during the growth of this compressional system (Figure 12b).

[27] Surface and subsurface data show that the structural architecture of the Sepa anticline and Paititi high are similar to the one of the Shira mountain, which may provide the Shira mountain is an inherited Early Carboniferous structure. Onlaps of the middle-upper Nia formations on the eastern limb of the Paititi high indicate small reactivation of this structure in Late Cretaceous times (Figure 12b). Such reactivation is also observed for several tectonic features in North Peru, Colombia and Venezuela [e.g., *Jaimes and de Freitas*, 2006]. No thickness variation in the Neogene sediments, which could support a synsedimentary Miocene uplift of the Shira mountain, is visible. However, the initiation of the Shira thrust system postdates the deposition of Pliocene-Pleistocene (?) strata (Figure 11).

[28] The role of Paleozoic compressional features has been previously described along the Andes from field observations [e.g., *Müller et al.*, 2002; *Jacobshagen et al.*, 2002; *Alvarez-Marron et al.*, 2006] and subsurface data [e.g., *Zubierta-Rossetti et al.*, 1993; *Colletta et al.*, 1997; *Vergés et al.*, 2007]. New evidence of such features in the Peruvian Subandes must be taken into account for their subsequent implications on the Neogene Subandean zone structural evolution of the Ene and southern Ucayali basins.

4. Regional Balanced Cross Sections

4.1. Principles of Construction

[29] In order to study the N-S trending evolution of the Ene and southern Ucayali basins, surface data, regional mapping, well information and seismic reflection data were integrated to construct two regional balanced cross sections, each of about 200 km long from the Eastern Cordillera to the Ucayali basin (Figure 2). The balanced cross sections were constructed according to thrust tectonic concepts [*Dahlstrom*, 1969; *Boyer and Elliott*, 1982; *Elliott*, 1983; *Woodward et al.*, 1985]. The cross sections were balanced using Midland Valley 2DMove 5.0 software on the basis of bed length and thickness conservation, and flexural-slip algorithm. The cross sections were restored at the bottom of the Late Cretaceous deposits, assuming that they were horizontal at deposition time, and pinned at local pin lines in the foreland. The cross section orientations are orthogonal to the fold axes, i.e., parallel to the inferred tectonic transport direction to minimize out-of-the-plane transport. Dip data have been projected onto sections along the fold axis directions [*Charlesworth et al.*, 1975].

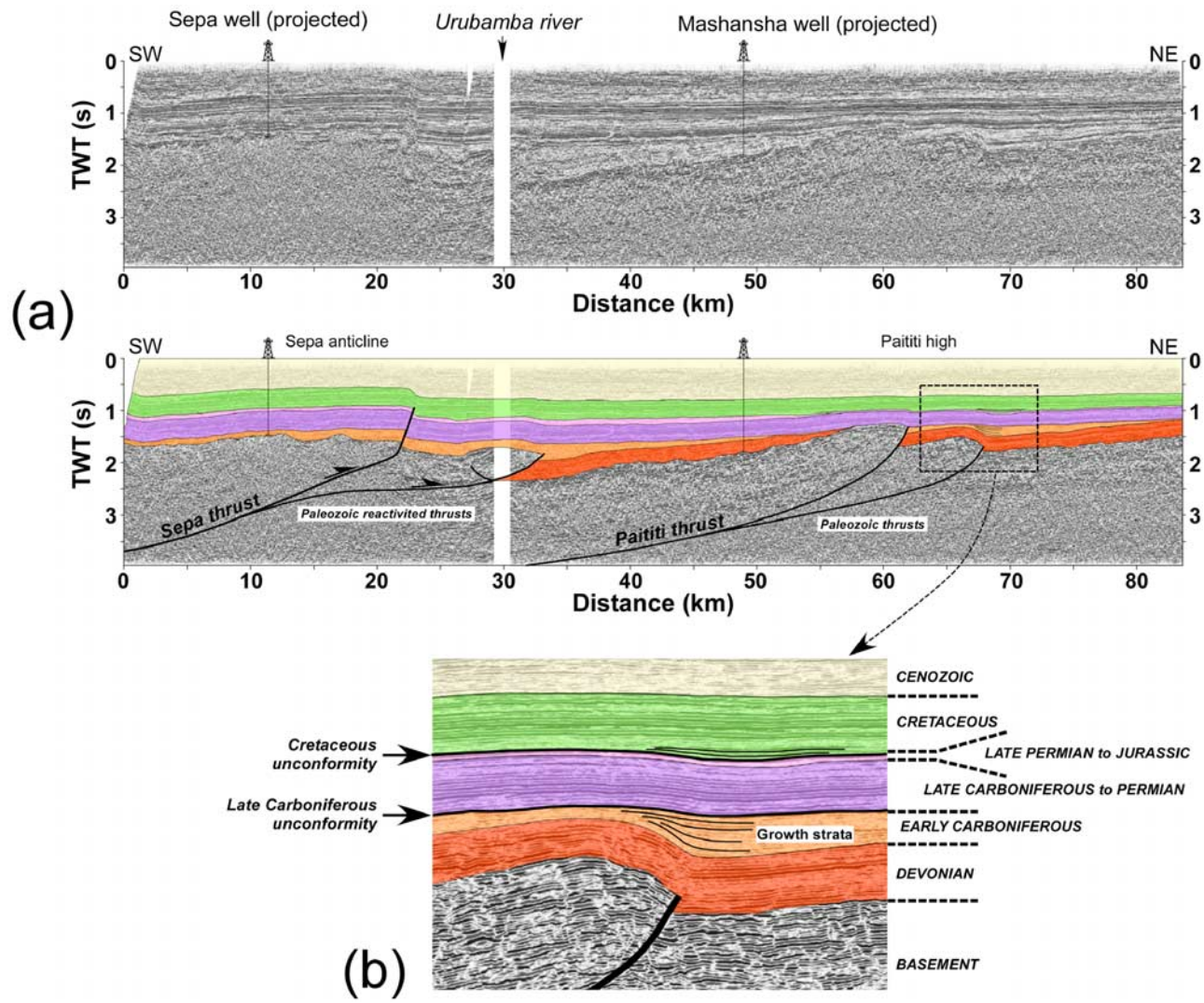

Figure 12. (a) Interpretation of seismic line 4 across the Sepa and Paititi high structures. For location, see Figures 2 and 10a. The reflectors have been calibrated using projected data of the Sepa and Mashansha wells. Faults are indicated by thick black lines. (b) Zoom on the Paititi high structure. Note the growth stratal pattern in the Early Carboniferous series (Ambo formation) on the eastern side of the Paititi high structure which recorded the activation of the thrust. TWT, two-way time.

4.2. Regional Balanced Cross Sections and Shortening Assessment

[30] The northern cross section A-A′ (Figures 2 and 13a) exhibits a narrow Subandean zone which is predominantly formed by the Ene basin (Figure 14a). The structural restoration shows that the western edge of the Ene basin corresponded to an extensional structure (Oxapampa-Satipo half-graben) during Permian-Triassic times. It was probably inverted during the beginning (Late Cretaceous) [*Baby et al.*, 1999; *Gil Rodriguez et al.*, 2001; *Hermoza et al.*, 2005; *Jaimes and de Freitas*, 2006] of the Andean compression and involved in the Subandean zone thrust system. It forms the boundary between the Eastern Cordillera and the Subandean zone. The cross section also shows that the geometry of the Ordovician-Devonian sedimentary prism controlled the deformation of the Subandean zone (Figure 14a). Thick Ordovician-Devonian sedimentary series are essentially restricted to the western side of the Shira mountain, thus preventing the eastward propagation of the Subandean thrust front (Figures 2 and 14a). Hence, the displacement is transferred deeper to the Early Carboniferous thick-skinned thrusts. The deep structure of the Shira mountain can be inferred from the dip of the eastern edge of the Ene basin. This dip can be controlled by a basement ramp underneath the Shira mountain. The regional structural cross section and subsurface data (Figures 11, 12, and 13a) argue in favor of a geodynamic model where the Shira mountain consists of two basement thrusts (Shira thrusts 1

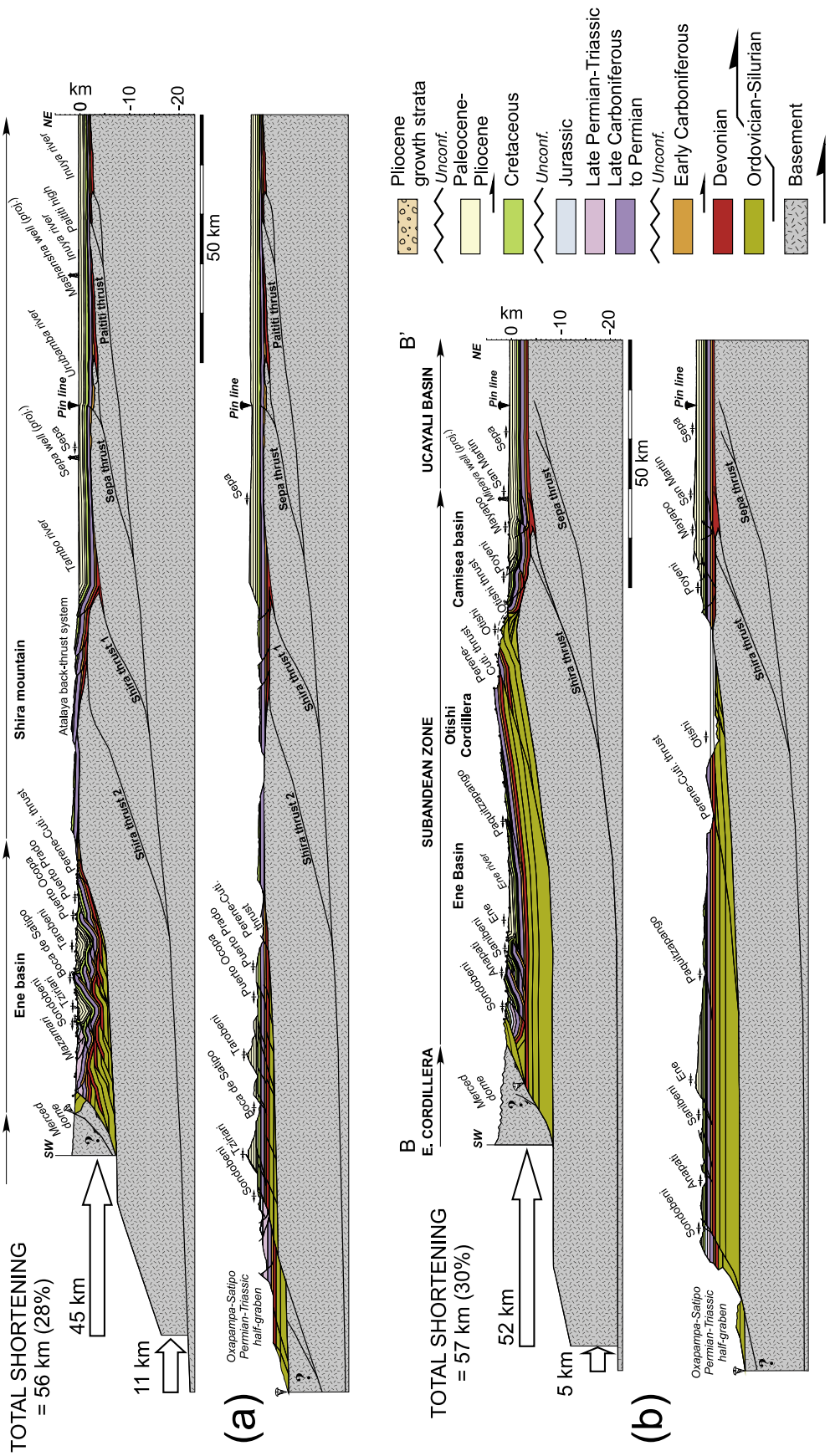

Figure 13. Regional balanced cross sections and restorations. For location, see Figure 2. Restored sections were obtained by flattening bottom of Late Cretaceous deposits. See construction method in the text. (a) Northern cross section A-A′ is formed by a N52°E western segment across the Eastern Cordillera, then the Ene basin along seismic line 1. N68°E central segment crosses the Shira mountain and the Atalaya back thrust system. N55°E eastern segment crosses the foreland along seismic line 4. (b) Southern cross section B-B′ is formed by a N75°E eastern segment across the Eastern Cordillera and the Ene basin. N50°E western segment crosses the Otishi Cordillera, and the Ucayali basin along seismic line 2.

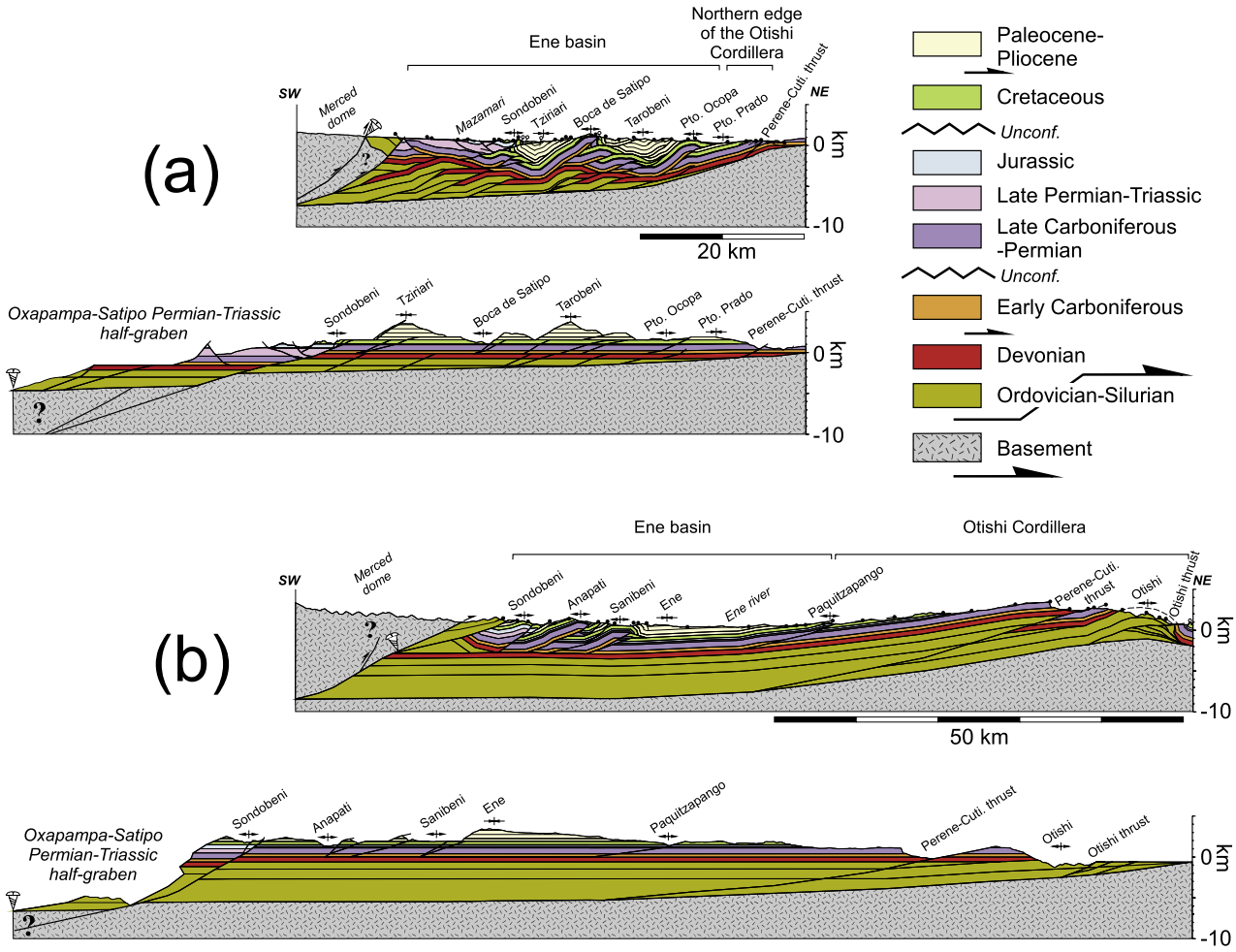

Figure 14. Details of the Subandean zone structure. The balanced and restored cross sections show evidence of thickness variations into the Paleozoic sedimentary series between the (a) northern and (b) southern Ene basin.

and 2; Figure 13a) which branch onto a west-dipping décollement located at about 18 km deep underneath the Ene basin. This geometry implies a vertical jump of displacement in the thick-skinned thrust system (Figure 13a).

[31] Cross section A-A′ shows a total shortening of ~56 km (28%). This shortening partitions vertically: 80% (i.e., 45 km) is accommodated into the Subandean zone and 20% (i.e., 11 km) is transferred into the thick-skinned thrust system (the Shira and Sepa thrusts) (Figure 13a).

[32] Southern cross section B-B′ (Figures 2 and 13b) shows that the Subandean thrust front is located 45 km easternmost than in the north (Figure 14b). As in section A-A′, the western edge of the section is formed by the Oxapampa-Satipo half-graben. The Ene basin is less deformed than in the north because the shortening is transferred eastward in the Otishi Cordillera thrust system (Figure 14b). Southward thickening of the Ordovician-Devonian sedimentary series (Figure 14b) is consistent with paleogeographic reconstructions of *Gil Rodriguez* [2002] where the Ordovician-Devonian sedimentary section exceeds 5 km thick southward. The envelope of the Otishi Cordillera outcropping thrusts allows us to infer a duplex structure below it. The Otishi Cordillera thrust system consists in a vertical stacking of four horses of Ordovician-Silurian rocks, what explains the high structural relief of the Otishi Cordillera. The Otishi duplex evolves northeastward into an imbricated fan thrust in the Camisea basin (Figure 13b). This imbricated fan branches onto the roof thrust of the Otishi duplex. Thus, the Otishi duplex shortening is transferred to the fore- and back-thrusts of the Camisea basin. As in the north, the sedimentary cover is detached northeastward above Early Carboniferous thick-skinned thrusts, reactivated during the Andean compression (Figure 13b). This thick-skinned thrust system determines the location of the Otishi Cordillera thrust system culmination, and it is interpreted as the southern continuation of the Shira thrust system. Thus, balanced cross section B-B′ was constructed assuming a ~18 km deep décollement beneath the Ene basin to respect the northern structural geometrical model of the section A-A′ (Figure 13a).

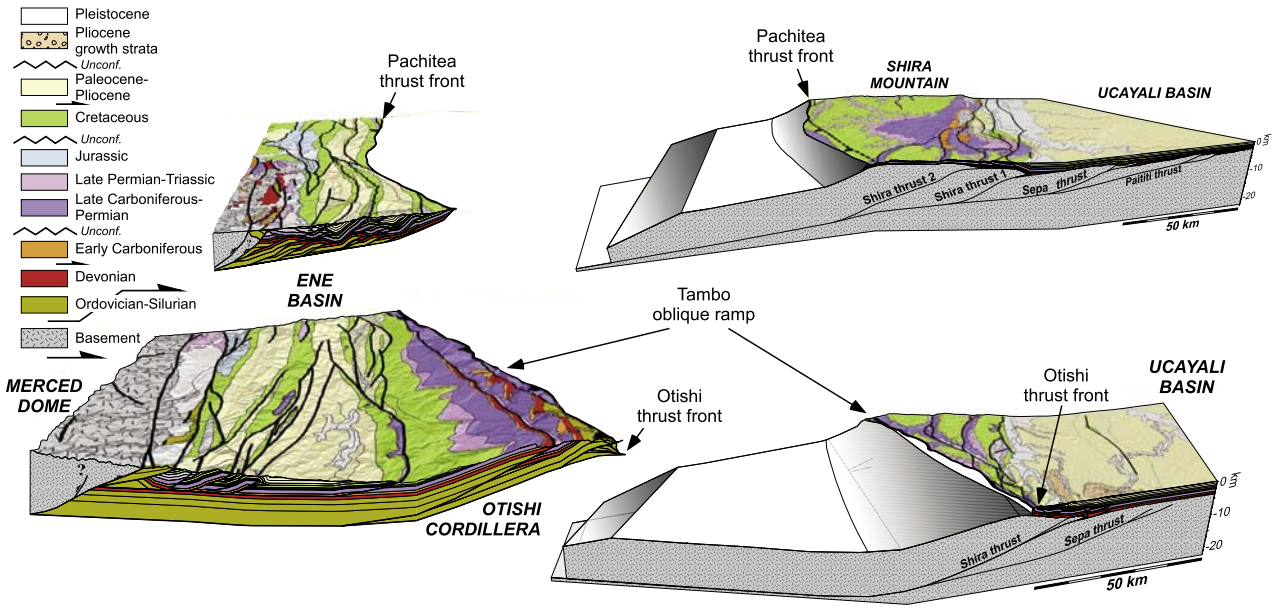

Figure 15. Three-dimensional diagram of the Ene and southern Ucayali basins with the two balanced cross sections showing the two stacked thrust wedges. The perspective view looking toward the north (with the upper thrust wedge to the west and the lower thrust wedge to the east). The geologic map of Figure 2 has been draped on the SRTM 90-m digital elevation model from NASA.

[33] Cross section B-B′ shows a total shortening of ~57 km (30%). In contrast to the northern section, 91% (i.e., 52 km) of the shortening is accommodated into the Subandean zone and only 9% (i.e., 5 km) is transferred within into thick-skinned thrust system (Shira thrust) (Figure 13b).

5. Discussion

[34] The balanced cross sections of the Ene and southern Ucayali foreland thrust belt show a vertical partitioning of the shortening, resulting from the kinematic linkage between two stacked thrust wedges: a lower thrust wedge involving the basement, and an upper thrust wedge, the Subandean zone, limited to the Paleozoic, Mesozoic, and Cenozoic sedimentary series (Figures 13 and 14). The lower thrust wedge is formed by thick-skinned thrusts which branch onto a west-dipping basal décollement (Figures 13, 14, and 15). This thick-skinned thrust system overprints Early Carboniferous low-angle thrust faults, which were eroded and then sealed by Late Carboniferous strata. That generated an irregular Paleozoic mechanical stratigraphy which controlled Neogene thrust propagation. The restoration of the balanced cross sections (Figure 13) shows that the Early Carboniferous thrust system of the Ucayali basin probably constituted the frontal part of a fold-and-thrust belt, as suggested by small thick-skinned thrust displacements. As a matter of fact, the southern Ucayali basin is not affected by the Permian-Triassic rift event [*Gil Rodriguez et al.*, 2001], what preserves the evidence of Paleozoic compressional features. The upper thrust wedge is characterized by thin-skinned style (Figures 13, 14, and 15). Thrust faults accommodate the major part of the shortening (80–90%) and the main décollement level is located at the interface between basement and Paleozoic sedimentary series.

[35] Along-strike thickness variations of the initial sedimentary series are expected to influence the geometry [e.g., *Marshak and Wilkerson*, 1992; *Calassou et al.*, 1993; *Boyer*, 1995; *Soto et al.*, 2002, 2003] and shortening gradient [e.g., *Baby et al.*, 1989; *Boyer*, 1995] of foreland thrust belts. Our balanced cross sections suggest that thickness variations of the Paleozoic sedimentary prism influenced the shortening gradient within the upper thrust wedge (Figures 13 and 16). To the north, the upper thrust wedge is restricted to the Ene basin. The thinning of the Ordovician-Devonian sedimentary prism prevented the large eastward propagation and shortening (45 km) of the upper thrust wedge and induced multiple tectonic imbricates and duplex structures within the northern Ene basin (Figures 13a and 14a). In contrast, the upper thrust wedge undergoes a maximum shortening (52 km) to the south (Figures 13b and 14b). The southward thickening of the Paleozoic sedimentary prism facilitated the eastward propagation of the upper thrust wedge leading to larger magnitude of thrusting and the development of the major Otishi Cordillera feature (Figure 16). Both restored cross sections show a same amount of overall shortening of ~56 km. Therefore, we propose that the calculated 7 km difference (16%) in displacement between the northern and southern upper thrust wedge was transferred onto the lower thrust wedge. To compensate such a difference, the transfer of displacement induced the reactivation of Early Carboniferous compressional structures in the Ucayali basin (Shira mountain and Sepa anticline) (Figure 16).

[36] The three-dimensional diagram of Figure 15 shows that the Otishi Cordillera uplift occurred along the Tambo

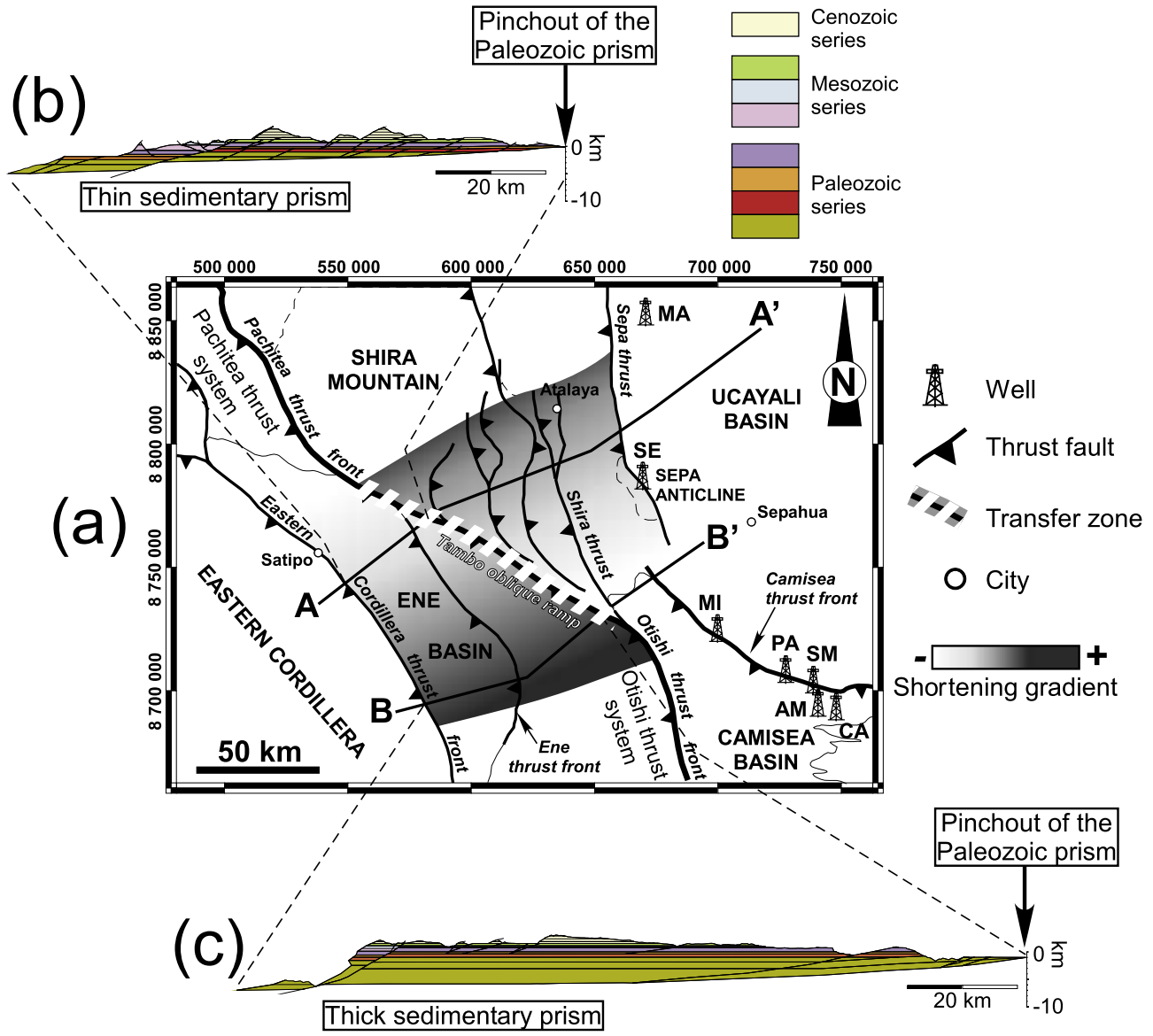

Figure 16. (a) Structural map of the Ene and southern Ucayali basins illustrating the spatial vertical partitioning of the shortening. Location of cross sections A-A′ and B-B′ are shown. The southward shortening gradient recorded in the upper thrust wedge (Subandean zone) is transferred northward in the lower thrust wedge (Shira mountain and Sepa anticline). This shortening transfer produced the development of the Tambo transfer zone between the Shira mountain and the Otishi Cordillera (dashed white area). Wells of the Ucayali basin are shown (MA, Mashansha; SE, Sepa; MI, Mipaya; PA, Pagoreni; SM, San Martin; AM, Armihuari; CA, Cashiriari). Restored geometries of the (b) northern and (c) southern sedimentary series are also shown. See the text for further discussions.

fault system which has the value of an oblique ramp. This oblique ramp constitutes a transfer zone between the Shira mountain and the Otishi Cordillera and links the southern end of the Pachitea thrust front to the Otishi thrust front (Figures 15 and 16). It developed along the pinchout of the Paleozoic sedimentary prism located onto the southwestern flank of the Shira mountain. The geometry of the Tambo oblique ramp in the Ucayali basin shows similar aspects with the Boomerang-Chapare transfer zone in the Bolivian Subandes, which led to a hundred kilometers of sinistral offset [*Baby et al.*, 1994]. In Bolivia, the loss of Subandean shortening to the north of the transfer zone seems to be compensated by increased shortening in the Interandean zone. In the Peruvian Subandes example, the presence of a foreland thick-skinned thrust system allowed to complete the N–S shortening assessment.

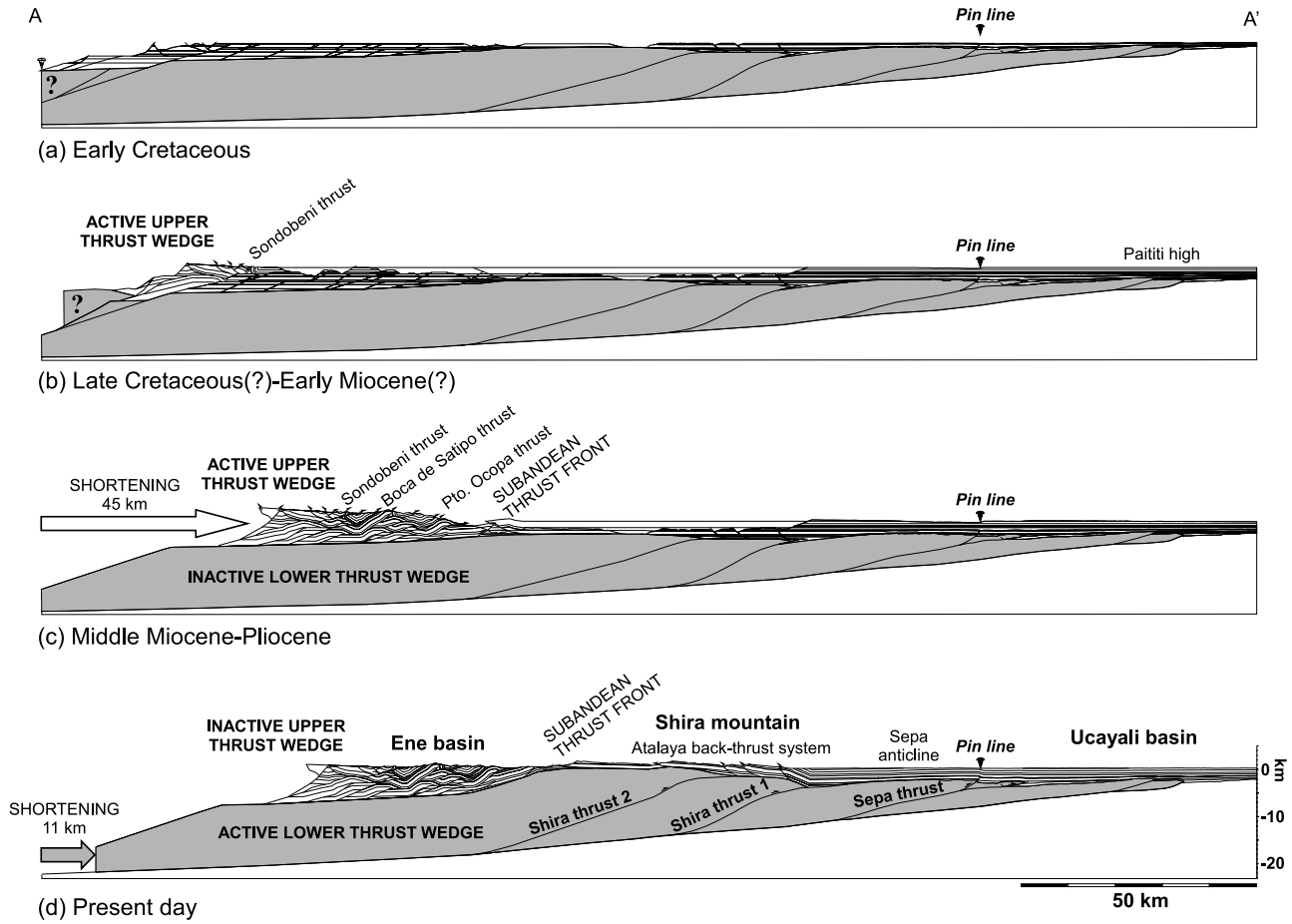

Figure 17. Kinematics evolution of the cross section A-A′ illustrating three stages of the thrust sequence. Grey areas indicate the lower thrust wedge and the open areas the upper thrust wedge. See details in the text.

[37] Thrust-top basins [e.g., *Butler and Grasso*, 1993; *Bonini et al.*, 1999] develop and fill during their displacement by active thrust sheets. On a large scale, thrust-top basins are promoted by the presence of a thick initial series inducing break-forward propagation of deformation far into the foreland [*Boyer*, 1992; *Leturmy et al.*, 2000]. The Ene basin presents a peculiar structural position in thrust-top basin between the Eastern Cordillera and the Otishi Cordillera (Figures 14, 15, and 16). To the north, the Ene basin disappears within the Pachitea thrust system. To the south, it abruptly disappears beneath the Eastern Cordillera thrust front. The basin deformation is directly controlled by the Tambo oblique ramp and developed on the thickest part of the Paleozoic sedimentary prism. The preservation of the Ene basin is associated with the development of the Otishi Cordillera, which resulted from the break-forward sequence of thrusts propagation.

[38] The relative timing of the upper and lower thrust wedges displacements can be indirectly interpreted from our structural analysis. Thus, a schematic deformation sequence can be proposed for cross section A-A′ (Figure 17). In the early stage (Late Cretaceous) of deformation, the inversion of the Oxapampa-Satipo half-graben occurred, and the Paititi high thrust was weakly reactivated (Figure 17b). Between 15 and 10 Ma [*Hermoza et al.*, 2005], the upper thrust wedge continued to propagate eastward (Figure 17c). It accommodated 45 km of shortening and the Subandean thrust front died out on the western side of the nonreactivated Shira thrust system. After motion on the upper thrust wedge ceased, the displacement continued deeper on the lower thrust wedge and Early Carboniferous thrusts reactivated. The 11 km of displacement were mainly accommodated in the Shira thrust system, prompting west-verging Atalaya back thrust system to form (Figure 17d). The displacement of the Shira thrust system was contemporaneous to the one of the southern Otishi thrust system. Consequently, synchronous along-strike motions of the Shira and the Otishi thrust systems produced the development of the Tambo transfer zone (Figure 15). The later Pliocene-Pleistocene (?) uplift of the Shira mountain caused tilting of the eastern edge of the Ene thrust-top basin.

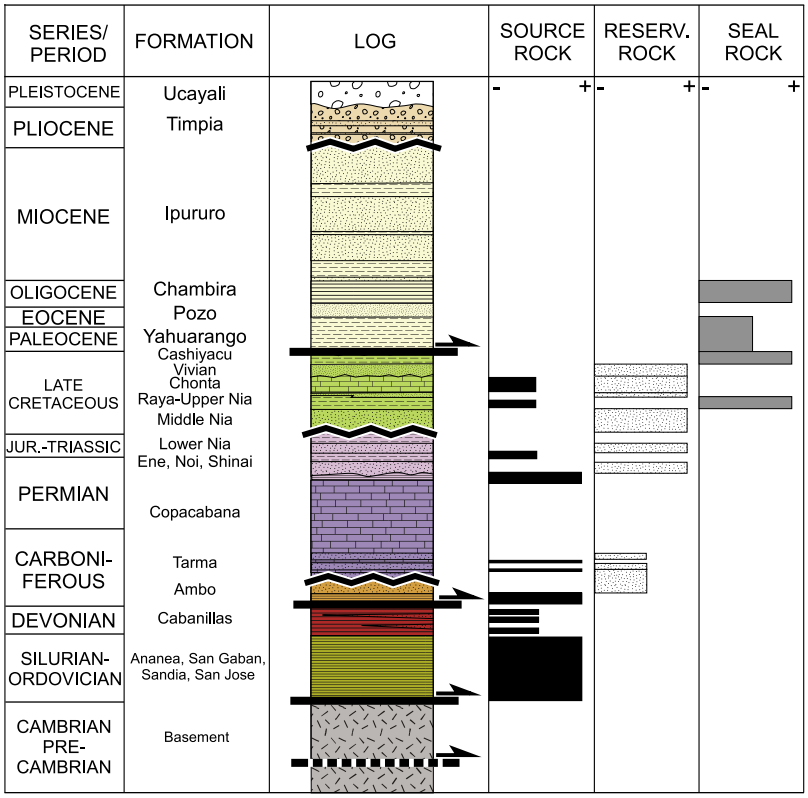

Figure 18. Petroleum system in the Ene and Camisea basins. See details in the text.

[39] In the study area, source rocks are essentially Paleozoic in age (Figure 18). The maturation and migration within Permian (Ene, Noi and lower Nia formations) and Cretaceous (upper Nia, Chonta and Vivian formations) reservoirs [*Chung et al.*, 2006] may have been controlled by the Neogene development of the Subandean zone, as observed in the Bolivian Subandes [e.g., *Baby et al.*, 1995; *Moretti et al.*, 1996]. North of the Tambo oblique ramp, Neogene sequences are less than 2 km thick [*Dumont et al.*, 1991]. Potential structural traps are only represented by thick-skinned structures and are not oil-bearing (Figure 16) [*Chung et al.*, 2006]. In contrast, east of Otishi thrust, the thin-skinned structures developed in the 5 km thick Neogene sequence, and produced structural traps of the Camisea hydrocarbon province (Figure 16) [*Chung et al.*, 2006; V. Graterol, unpublished report, 1998]. The vertical partitioning of thrust deformation may explain the presence of hydrocarbons in the structural traps of the upper thrust wedge. The thin-skinned tectonic style might be linked to a maximum thickness of the Neogene sedimentary series. In return, thick Neogene sedimentary series might have controlled the petroleum system and hydrocarbon migration toward thin-skinned structures. Hence, the petroleum play extension of the giant gas/condensate province of the Camisea basin (Figures 2 and 18) may be found in the poorly explored Ene basin, which may have favorable timing of trap formation and hydrocarbon generation [*Fabre and Alvarez*, 1993]. Consequently, the Tambo transfer zones play an important role for oil and gas field location. The modern structural configuration of the Neogene Ene basin may constitute a key area for future hydrocarbon exploration in the Peruvian Subandes.

6. Conclusions

[40] Surface and subsurface data together with the construction of two regional balanced cross sections have been integrated to study the structural architecture, kinematics and mechanism of the deformation of the Ene and southern Ucayali basins. The main conclusions are as follows.

[41] 1. The southern Ucayali basin exhibits Early Carboniferous thick-skinned thrusts, eroded and then sealed during the Late Carboniferous.

[42] 2. The Neogene shortening of the Ucayali Subandean zone was vertically partitioned into two stacked thrust wedges: a lower duplex system controlled by reactivated Early Carboniferous thick-skinned thrusts, and an upper thrust wedge, the Subandean zone (Ene basin, Otishi Cordillera and Camisea basin), essentially driven by a thin-skinned thrusts.

[43] 3. The shortening within the upper thrust wedge is governed by thickness variations of the Paleozoic sedimentary series. The maximum of shortening is observed southward where the Paleozoic sedimentary series is the most developed. Northward, the thickness of Paleozoic sedimentary series decreases and the shortening has been transferred in the lower thrust wedge. The kinematic linkage of the two

thrust wedges contributed to a N-S complete shortening assessment (~56 km).

[44] 4. The Tambo fault system is an oblique ramp developed on the northeastern pinchout of the Ordovician-Devonian sedimentary series. This is a regional transfer zone which expresses the relative displacement between the two stacked thrust wedges.

[45] 5. The maximum thickness of the Neogene sedimentary series might be structurally controlled by the thin-skinned tectonic style of the upper thrust wedge. In return, thick Neogene sedimentary might have controlled the petroleum system. Thus, the unexplored and preserved Ene basin evolving on the upper thrust wedge may constitute a structural key area for future hydrocarbon exploration in the Peruvian Subandes.

[46] **Acknowledgments.** This research project was led thanks to the Institut de Recherche pour le Développement–PERUPETRO S.A.–PLUSPETROL E&P S.A. research agreement, and supported by IRD (UR 154) and French INSU–CNRS programs DyETI (Dynamique et Evolution de la Terre Interne) and ECLIPSE II (Environnement et CLImat du Passé: hiStoire et Evolution). We thank PERUPETRO S.A. for providing seismic reflection profiles and for permissions to publish their imagery. Midland Valley is acknowledged for providing "2DMove" for kinematic structural modeling. We also thank G. Bessereau, J.C. Soula, and M. Espurt for their useful comments and suggestions. We finally thank reviewers O. Oncken and P. Cobbold for their interesting comments that helped to improve the paper.

References

Alvarez-Marron, J., R. Rodriguez-Fernandez, N. Heredia, P. Busquets, F. Colombo, and D. Brown (2006), Neogene structures overprinting Palaeozoic thrust system in the Andean Precordillera at 30°S latitude, *J. Geol. Soc.*, *163*, 949–964, doi:10.1144/0016-76492005-142.

Baby, P., G. Hérail, M. López, O. López, J. Oller, J. Pareja, T. Sempere, and D. Tufiño (1989), Structure de la zone subandine de Bolivie: Influence de la géométrie des séries sédimentaires antéorogéniques sur la propagation des chevauchements, *C. R. Acad. Sci., Ser. II*, *309*, 1717–1722.

Baby, P., G. Hérail, R. Salinas, and T. Sempere (1992), Geometry and kinematic evolution of passive roof duplexes deduced from cross section balancing: Example from the foreland thrust system of the southern Bolivian Subandean zone, *Tectonics*, *11*, 523–536, doi:10.1029/91TC03090.

Baby, P., M. Specht, J. Oller, G. Montemurro, B. Colletta, and J. Letouzey (1994), The Boomerang-Chapare transfer zone (recent oil discovery trend in Bolivia): Structural interpretation and experimental approach, in *Geodynamic Evolution of Sedimentary Basins: EAPG Congress, Moscow*, edited by F. Roure, V. S. Shein, and I. Skvortsov, pp. 203–218, Technip Ed., Paris.

Baby, P., I. Moretti, B. Guillier, R. Limachi, E. Mendez, J. Oller, and M. Specht (1995), Petroleum system of the northern and central Bolivian sub-Andean zone, in *Petroleum Basins of South America*, edited by A. J. Tankard, R. Suarez, and H. J. Welsink *Mem. Am. Assoc. Pet. Geol.*, *62*, 445–458.

Baby, P., M. Rivadeneira, F. Christophoul, and R. Barragan (1999), Style and timing of deformation in the Oriente Basin of Ecuador, paper presented at Fourth International Symposium on Andean Geodynamics (ISAG'99), Univ. Göttingen, Göttingen, Germany.

Ballard, J. F., F. Cerda, J. C. Guillon, H. Pourtal, and J. F. Riou (1997), Peru-Block 66 geological synthesis: Structural geology, *Elf Rep. Tech. Arch. ITP 20010*, PeruPetro, Lima.

Bellido, B. E. (1969), Sinopsis de la geología del Perú, *Serv. Geol. Miner. Bol.*, *22*, 54 pp.

Benavides, V. (1956), Cretaceous system in northern Perú, *Bull. Am. Mus. Nat. Hist.*, *108*, 352–494.

Bonini, M., G. Moratti, and F. Sani (1999), Evolution and depocentre migration in thrust-top basins: Inferences from the Messinian Velona Basin (Northern Apennines, Italy), *Tectonophysics*, *304*, 95–108, doi:10.1016/S0040-1951(98)00291-1.

Boyer, S. E. (1992), Geometric evidence for synchronous thrusting in the southern Alberta and northwest Montana thrust belts, in *Thrust Tectonics*, edited by K. R. McClay, pp. 377–390, Chapman and Hall, London.

Boyer, S. E. (1995), Sedimentary basin taper as a factor controlling the geometry and advance of thrust belts, *Am. J. Sci.*, *295*, 1220–1254.

Boyer, S. E., and D. Elliott (1982), The geometry of thrust systems, *AAPG Bull.*, *66*, 1196–1230.

Butler, R. W. H., and M. Grasso (1993), Tectonic controls on base-level variations and depositional sequences within thrust-top and foredeep basins: Examples from the Neogene thrust belt of central Sicily, *Basin Res.*, *5*, 137–151, doi:10.1111/j.1365-2117.1993.tb00062.x.

Cabrera La Rosa, A., and G. Petersen (1936), Reconocimiento geologico de los yacimientos petroliferos del Departamento de Puno, *Bol. Cuerpo Ing. Minas Peru*, *115*, 1–110.

Calassou, S., C. Larroque, and J. Malavieille (1993), Transfer zones of deformation in thrust wedges: An experimental study, *Tectonophysics*, *221*, 325–344, doi:10.1016/0040-1951(93)90165-G.

Capdevila, R., F. Mégard, J. Parades, and P. H. Vidal (1977), Le batholite de San Ramon (Cordillière Orientale du Pérou central). Un granite hercynien mis en place à la limite Permien-Trias. Données géologiques et radiométriques, *Geol. Rundsch.*, *66*, 434–446, doi:10.1007/BF01989586.

Charlesworth, H. A. K., C. W. Langenberg, and J. Ramsden (1975), Determining axes, axial planes, and sections of macroscopic folds using computer-based methods, *Can. J. Earth Sci.*, *13*, 54–65.

Chung, J., M. Arteaga, S. Davis, and F. Seminario (2006), Impacto de la sismica 3D en el desarrollo de los yacimientos de Camisea, Bloque 88–Cuenca Ucayali–Peru, *Bol. Soc. Geol. Peru*, *101*, 73–89.

Cobbold, P. R., E. A. Rossello, P. Roperch, C. Arriagada, L. A. Gomez, and C. Lima (2007), Distribution, timing, and causes of Andean deformation across South America, in *Deformation of the Continental Crust: The Legacy of Mike Coward*, edited by A. C. Ries, R. W. H. Butler, and R. H. Graham, *Geol. Soc. Spec. Publ.*, *272*, 321–343.

Colletta, B., F. Roure, B. De Toni, D. Loureiro, H. Passalacqua, and Y. Gou (1997), Tectonic inheritance, crustal architecture, and contrasting structural style in the Venezuelan Andes, *Tectonics*, *16*, 777–794, doi:10.1029/97TC01659.

Corrado, S., D. Di Bucci, G. Naso, and C. Faccenna (1998), Influence of palaeogeography on thrust system geometries: An analogue modeling approach for the Abruzzi–Molise (Italy) case history, *Tectonophysics*, *296*, 437–453, doi:10.1016/S0040-1951(98)00147-4.

Dahlstrom, C. D. A. (1969), Balanced cross sections, *Can. J. Earth Sci.*, *6*, 743–757.

Dalmayrac, B., G. Laubacher, and R. Marocco (1980), Caractères généraux de l'évolution géologique des Andes Péruviennes, *Travaux Doc. 122*, 501 pp., Inst. Fr. de Rech. Sci. pour le Dev. en Coop. (ORSTOM), Paris.

Dorbath, C. (1996), Velocity structure of the Andes of central Peru from locally recorded earthquakes, *Geophys. Res. Lett.*, *23*, 205–208, doi:10.1029/95GL03778.

Dumont, J. F., E. Deza, and F. Garcia (1991), Morphostructural provinces and neotectonics in the Amazonian lowlands of Peru, *J. S. Am. Earth Sci.*, *4*, 373–381, doi:10.1016/0895-9811(91)90008-9.

Dunbar, C. O., and N. D. Newell (1946), Marine early Permian of the Central Andes and its fusuline faunas, *Am. J. Sci.*, *244*, 377–402, 457–491.

Elliott, D. (1983), The construction of balanced cross sections, *J. Struct. Geol.*, *5*, 101, doi:10.1016/0191-8141(83)90035-4.

Espurt, N., P. Baby, S. Brusset, M. Roddaz, W. Hermoza, V. Regard, P.-O. Antoine, R. Salas-Gismondi, and R. Bolaños (2007), How does the Nazca Ridge subduction influence the modern Amazonian foreland basin?, *Geology*, *35*, 515–518, doi:10.1130/G23237A.1.

Fabre, A. D., and D. U. Alvarez (1993), The hydrocarbon potential of the Ene Basin (Peru), *AAPG Bull.*, *77*, abstract CONF-930306.

Giambiagi, L. B., V. A. Ramos, E. Godoy, P. P. Alvarez, and S. Orts (2003), Cenozoic deformation and tectonic style of the Andes, between 33° and 34° south latitude, *Tectonics*, *22*(4), 1041, doi:10.1029/2001TC001354.

Gil Rodriguez, W. (2002), Evolución lateral de la deformación de un frente orogénico: Ejemplo de las cuencas subandinas entre 0°y 16°S, *Publ. Espec.*, *4*, 146 pp., Soc. Geol. de Peru, Lima.

Gil Rodriguez, W., P. Baby, and J. F. Ballard (2001), Structure et contrôle paléogéographique de la zone subandine péruvienne, *C. R. Acad. Sci., Ser. II*, *333*, 741–748.

Gripp, A. E., and R. G. Gordon (2002), Young tracks of hotspots and current plate velocities, *Geophys. J. Int.*, *150*, 321–361, doi:10.1046/j.1365-246X.2002.01627.x.

Gutscher, M.-A., J.-L. Olivet, D. Aslanian, J. P. Eissen, and R. Maury (1999), The "lost Inca Plateau": Cause of flat subduction beneath Peru?, *Earth Planet. Sci. Lett.*, *171*, 335–341, doi:10.1016/S0012-821X(99)00153-3.

Hermoza, W., S. Brusset, P. Baby, W. Gil, M. Roddaz, N. Guerrero, and R. Bolaños (2005), The Huallaga foreland basin evolution: Thrust propagation in a deltaic environment, northern Peruvian Andes, *J. S. Am. Earth Sci.*, *19*, 21–34, doi:10.1016/j.jsames.2004.06.005.

Hinsch, R., C. M. Krawczyk, C. Gaedicke, R. Giraudo, and D. Demuro (2002), Basement control on oblique thrust sheet evolution: Seismic imaging of the active deformation front of the Central Andes in Bolivia, *Tectonophysics*, *355*, 23–39, doi:10.1016/S0040-1951(02)00132-4.

Houzay, J. P., and C. Sejourne (1997), Peru-Block 66 organic geochemistry study petroleum system: Description and behaviour 1996 and up to date, *Elf Rep. Tech. Arch. ITP 20014*, PeruPetro, Lima.

Jacobshagen, V., J. Müller, K. Wemmer, H. Ahrendt, and E. Manutsoglu (2002), Hercynian deformation

and metamorphism in the Cordillera Oriental of southern Bolivia, central Andes, *Tectonophysics*, *345*, 119–130, doi:10.1016/S0040-1951(01)00209-8.

Jaffuel, F. (1997), Peru-Block 66 geological synthesis: Inorganic geochemistry, *Elf Rep. Tech. Arch. ITP 20012*, PeruPetro, Lima.

Jaimes, E., and M. de Freitas (2006), An Albian-Cenomanian unconformity in the northern Andes: Evidence and tectonics significance, *J. S. Am. Earth Sci.*, *21*, 466–492, doi:10.1016/j.jsames.2006.07.011.

Kley, J. (1996), Transition from basement-involved to thin-skinned thrusting in the. Cordillera Oriental of southern Bolivia, *Tectonics*, *15*, 763–775, doi:10.1029/95TC03868.

Kley, J., C. R. Monaldi, and J. A. Salfity (1999), Along-strike segmentation of the Andean foreland: Causes and consequences, *Tectonophysics*, *301*, 75–94, doi:10.1016/S0040-1951(98)90223-2.

Koch, E. (1962), Die Tektonik im Subandin des Mittel-Ucayali-Gebietes, Ost-Peru, *Geotekt. Forsch.*, *15*, 67 pp.

Kummel, B. (1948), Geological reconnaissance of the Contamana region, Peru, *Geol. Soc. Am. Bull.*, *59*, 1217–1266, doi:10.1130/0016-7606(1948)59[1217:GROTCR]2.0.CO;2.

Lacombe, O., and F. Mouthereau (2002), Basement-involved shortening and deep detachment tectonics in forelands of orogens: Insights from recent collision belts (Taiwan, Western Alps, Pyrenees), *Tectonics*, *21*(4), 1030, doi:10.1029/2001TC901018.

Laubacher, G., and C. W. Naeser (1994), Fission-track dating of granitic rocks from the Eastern Cordillera of Peru: Evidence for Late Jurassic and Cenozoic cooling, *J. Geol. Soc.*, *151*, 473–483, doi:10.1144/gsjgs.151.3.0473.

Leturmy, P., J. L. Mugnier, P. Vinour, P. Baby, B. Colletta, and E. Chabron (2000), Piggyback basin development above a thin-skinned thrust belt with two detachment levels as a function of interactions between tectonic and superficial mass transfer: The case of the Subandean Zone (Bolivia), *Tectonophysics*, *320*, 45–67, doi:10.1016/S0040-1951(00)00023-8.

Marques, F. O., and P. R. Cobbold (2002), Topography as a major factor in the development of arcuate thrust belts: Insights from sandbox experiments, *Tectonophysics*, *348*, 247–268, doi:10.1016/S0040-1951(02)00077-X.

Marshak, S., and M. S. Wilkerson (1992), Effect of overburden thickness on thrust belt geometry and development, *Tectonics*, *11*, 560–566, doi:10.1029/92TC00175.

Mathalone, J. M. P., and R. M. Montoya (1995), Petroleum geology of sub-Andean basins of Peru, in *Petroleum Basins of South America*, edited by A. Tankard, R. S. Soruco, and H. J. Welsink, *AAPG Mem.*, *62*, 423–444.

McClelland, W. C., and J. S. Oldow (2004), Displacement transfer between thick- and thin-skinned décollement systems in the central North American Cordillera, in *Vertical Coupling and Decoupling in the Lithosphere*, edited by J. Grocott et al., *Geol. Soc. Spec. Publ.*, *227*, 177–195.

McQuarrie, N. (2004), Crustal scale geometry of the Zagros fold–thrust belt, Iran, *J. Struct. Geol.*, *26*, 519–535, doi:10.1016/j.jsg.2003.08.009.

Mégard, F. (1978), Etude géologique des Andes du Pérou central: Contribution à l'étude géologique des Andes n°1, *Mem. Orstom*, *86*, 310 pp., Inst. Fr. de Rech. Sci. pour le Dev. en Coop. (ORSTOM), Paris.

Mégard, F. (1979), Estúdio geológico de los Andes del Perú central, *Bol. Inst. Geol. Min. Met., Ser. D*, *8*, 207–227.

Mitra, S. (1990), Fault-propagation folds: Geometry, kinematic evolution, and hydrocarbon traps, *Am. Assoc. Pet. Geol. Bull.*, *74*, 921–945.

Mon, R., C. R. Monaldi, and J. A. Salfity (2005), Curved structures and interference fold patterns associated with lateral ramps in the Eastern Cordillera, Central Andes of Argentina, *Tectonophysics*, *399*, 173–179, doi:10.1016/j.tecto.2004.12.021.

Moretti, I., P. Baby, E. Mendez, and D. Zubieta (1996), Hydrocarbon generation in relation to thrusting in the Sub Andean Zone from 18 to 22°S, Bolivia, *Mar. Pet. Geol.*, *2*, 17–26.

Mouthereau, F., O. Lacombe, B. Deffontaines, J. Angelier, H. T. Chu, and C. T. Lee (1999), Quaternary transfer faulting and belt front deformation at Pakuashan (western Taiwan), *Tectonics*, *18*, 215–230, doi:10.1029/1998TC900025.

Mueller, K., and P. Talling (1997), Geomorphic evidence for tear faults accommodating lateral propagation of an active fault-bend fold, Wheeler Ridge, California, *J. Struct. Geol.*, *19*, 397–411, doi:10.1016/S0191-8141(96)00089-2.

Müller, J. P., J. Kley, and V. Jacobshagen (2002), Structure and Cenozoic kinematics of the Eastern Cordillera, southern Bolivia (21°S), *Tectonics*, *21*(5), 1037, doi:10.1029/2001TC001340.

Newell, N. D., J. Chronic, and T. Robert (1953), Upper Paleozoic of Peru, *Mem. Geol. Soc. Am.*, *58*, 256 pp.

Philippe, Y., E. Deville, and A. Mascle (1998), Thin-skinned inversion tectonics at oblique basin margins: Example of the western Vercors and Chartreuse Subalpine massifs (SE France), in *Cenozoic Foreland Basins of Western Europe*, edited by A. Mascle et al., *Geol. Soc. Spec. Publ.*, *134*, 239–262.

Räsänen, M. E., J. S. Salo, and R. J. Kalliola (1987), Fluvial perturbance in the Western Amazon Basin: Regulation by long-term Sub-Andean tectonics, *Science*, *238*, 1398–1401, doi:10.1126/science.238.4832.1398.

Ravaglia, A., C. Turrini, and S. Seno (2004), Mechanical stratigraphy as a factor controlling the development of a sandbox transfer zone: A three-dimensional analysis, *J. Struct. Geol.*, *26*, 2269–2283, doi:10.1016/j.jsg.2004.04.009.

Roddaz, M., J. Viers, S. Brusset, P. Baby, and G. Hérail (2005), Sediment provenances and drainage evolution of the Neogene Amazonian foreland basin, *Earth Planet. Sci. Lett.*, *239*, 57–78, doi:10.1016/j_enh.epsl.2005.08.007.

Rosas, S., L. Fontboté, and A. Tankard (2007), Tectonic evolution and paleogeography of the Mesozoic Pucará Basin, central Peru, *J. S. Am. Earth Sci.*, *24*, 1–24, doi:10.1016/j.jsames.2007.03.002.

Seminario, F., and J. Guizado (1976), Síntesis biestratigrafica de la region de la Selva del Peru, in *Congreso Latinoamericano de Geologia, 2, Caracas, 1973, Memoria*, Sucre, Caracas.

Shaw, J. H., F. Bilotti, and P. A. Brennan (1999), Patterns of imbricate thrusting, *Geol. Soc. Am. Bull.*, *111*, 1140–1154, doi:10.1130/0016-7606(1999)111<1140:POIT>2.3.CO;2.

Sherkati, S., M. Molinaro, D. Frizon de Lamotte, and J. Letouzey (2005), Detachment folding in the Central and Eastern Zagros fold-belt (Iran): Salt mobility, multiple detachments and late basement control, *J. Struct. Geol.*, *27*, 1680–1696, doi:10.1016/j.jsg.2005.05.010.

Smith, H. F. W., and D. T. Sandwell (1997), Global sea floor topography from satellite altimetry and ship depth soundings, *Science*, *277*, 1956–1961, doi:10.1126/science.277.5334.1956.

Soler, P., and M. G. Bonhomme (1987), Données radiochronologiques K-Ar sur les granitoïdes de la Cordillère orientale des Andes du Pérou central, Implications tectoniques, *C. R. Acad. Sci., Ser. II*, *304*, 841–845.

Soler, P., and M. G. Bonhomme (1990), Relation of magmatic activity to plate dynamics in central Peru from Late Cretaceous to present, *Spec. Pap. Geol. Soc. Am.*, *241*, 173–192.

Soto, R., A. M. Casas, F. Storti, and C. Faccenna (2002), Role of lateral thickness variations on the development of oblique structures at the western end of the South Pyrenean Central Unit, *Tectonophysics*, *350*, 215–235, doi:10.1016/S0040-1951(02)00116-6.

Soto, R., F. Storti, A. M. Casas, and C. Faccenna (2003), Influence of along-strike pre-orogenic sedimentary tapering on the internal architecture of experimental thrust wedges, *Geol. Mag.*, *140*, 253–264, doi:10.1017/S0016756803007817.

Suppe, J., and D. A. Medwedeff (1990), Geometry and kinematics of fault-propagation folding, *Eclogae Geol. Helv.*, *83*(3), 409–454.

Szekely, T. S., and L. T. Grose (1972), Stratigraphy of the carbonate, black shale and phosphate of the Pucara Group (Upper Triassic(Lower Jurassic), Central Andes, Peru, *Geol. Soc. Am. Bull.*, *83*, 407–428, doi:10.1130/0016-7606(1972)83[407:SOTCBS]2.0.CO;2.

Thomas, W. A. (1990), Controls on locations of transverse zones in thrusts belts, *Eclogae Geol. Helv.*, *83*, 727–744.

Vergés, J., V. A. Ramos, A. Meigs, E. Cristallini, F. H. Bettini, and J. M. Cortés (2007), Crustal wedging triggering recent deformation in the Andean thrust front between 31°S and 33°S: Sierras Pampeanas-Precordillera interaction, *J. Geophys. Res.*, *112*, B03S15, doi:10.1029/2006JB004287.

Wang, E. (1997), Displacement and timing along the northern strand of the Altin Tagh fault zone, northern Tibet, *Earth Planet. Sci. Lett.*, *150*, 55–64, doi:10.1016/S0012-821X(97)00085-X.

Wilkerson, M. S., T. Apotria, and T. Farid (2002), Interpreting the geologic map expression of contractional fault-related fold terminations: Lateral/oblique ramps versus displacement gradient, *J. Struct. Geol.*, *24*, 593–607, doi:10.1016/S0191-8141(01)00111-0.

Williams, M. D. (1949), Depositos terciarios continentales del Valle del Alto Amazonas, *Bol. Soc. Geol. Peru*, *XXV*, 15 pp.

Wilson, J. J., and L. Reyes (1964), Geología del Cuadrángulo de Pataz, *Bol. Inst. Geol. Miner. Metal., Ser. A*, *9*, 91 pp.

Woodward, N. B., S. E. Boyer, and J. Suppe (1985), *An Outline of Balanced Cross Sections*, 2nd ed., *Stud. Geol.*, vol. 11 Dep. of Geol., Univ. of Tenn., Knoxville.

Zubierta-Rossetti, D., P. Huyghe, G. Mascle, J.-L. Mugnier, and P. Baby (1993), Influence de l'héritage anté-dévonien au front de la chaîne andine (Partie centrale de la Bolivie), *C. R. Acad. Sci., Ser. II*, *316*, 951–957.

P. Baby, S. Brusset, and J. Déramond, Laboratoire des Mécanismes et Transferts en Géologie, Université de Toulouse, CNRS, IRD, OMP, 14 Av. East Belin, F-31400 Toulouse, France.

R. Bolaños, PERUPETRO S.A., Av. Luis Aldana 320, San Borja, Lima 41, Peru.

N. Espurt, Institut Français du Pétrole, 1 et 4 Av. de Bois-Préau, 92852 Rueil-Malmaison CEDEX, France. (nicolas.espurt@ifp.fr)

M. Hermoza, REPSOL-YPF, Paseo de la Castellana 280, 1a Pl., E-28046 Madrid, Spain.

D. Uyen, PLUSPETROL E&P S.A., Av. Republica de Panama 3055, San Isidro, Lima 27, Peru.